The Plant Cell, Vol. 28: 537–556, February 2016, www.plantcell.org

Pectin Biosynthesis Is Critical for Cell Wall Integrity and Immunity in *Arabidopsis thaliana*

Gerit Bethke,[a,1] Amanda Thao,[a] Guangyan Xiong,[b,2] Baohua Li,[c] Nicole E. Soltis,[c] Noriyuki Hatsugai,[a] Rachel A. Hillmer,[a,d] Fumiaki Katagiri,[a] Daniel J. Kliebenstein,[c] Markus Pauly,[b,e] and Jane Glazebrook[a]

[a] Department of Plant Biology, University of Minnesota, St. Paul, Minnesota 55108
[b] Energy Biosciences Institute, University of California, Berkeley, California 94720
[c] Department of Plant Sciences, University of California, Davis, California 95616
[d] Plant Biological Sciences Graduate Program, University of Minnesota, St. Paul, Minnesota 55108
[e] Department of Plant and Microbial Biology, University of California, Berkeley, California, 94720

ORCID IDs: 0000-0001-7235-0470 (B.L.); 0000-0001-9213-9904 (N.E.S.); 0000-0003-0632-5597 (R.A.H.); 0000-0001-5759-3175 (D.J.K.); 0000-0001-5167-736X (J.G.)

Plant cell walls are important barriers against microbial pathogens. Cell walls of *Arabidopsis thaliana* leaves contain three major types of polysaccharides: cellulose, various hemicelluloses, and pectins. UDP-D-galacturonic acid, the key building block of pectins, is produced from the precursor UDP-D-glucuronic acid by the action of glucuronate 4-epimerases (GAEs). *Pseudomonas syringae* pv *maculicola* ES4326 (*Pma* ES4326) repressed expression of *GAE1* and *GAE6* in Arabidopsis, and immunity to *Pma* ES4326 was compromised in *gae6* and *gae1 gae6* mutant plants. These plants had brittle leaves and cell walls of leaves had less galacturonic acid. Resistance to specific *Botrytis cinerea* isolates was also compromised in *gae1 gae6* double mutant plants. Although oligogalacturonide (OG)-induced immune signaling was unaltered in *gae1 gae6* mutant plants, immune signaling induced by a commercial pectinase, macerozyme, was reduced. Macerozyme treatment or infection with *B. cinerea* released less soluble uronic acid, likely reflecting fewer OGs, from *gae1 gae6* cell walls than from wild-type Col-0. Although both OGs and macerozyme-induced immunity to *B. cinerea* in Col-0, only OGs also induced immunity in *gae1 gae6*. Pectin is thus an important contributor to plant immunity, and this is due at least in part to the induction of immune responses by soluble pectin, likely OGs, that are released during plant-pathogen interactions.

INTRODUCTION

The cell walls in *Arabidopsis thaliana* leaves are mainly primary cell walls consisting of three major types of polysaccharides—cellulose, various hemicelluloses, and various pectic polysaccharides—as well as some structural proteins (Liepman et al., 2010). Arabidopsis leaf walls contain ~14% cellulose, a homopolymer of (1,4)-β linked D-glucose subunits (Zablackis et al., 1995; Carpita, 2011). Hemicelluloses are a diverse class of polysaccharides that includes xylans, xyloglucans, mannans, glucomannans, and mixed-linkage β-glucans (Scheller and Ulvskov, 2010). In Arabidopsis leaves, the major hemicellulose is xyloglucan, which constitutes ~20% of the wall polysaccharides. Xyloglucan contains a (1,4)-β-linked glucan backbone substituted with (1,6)-α-linked xylosyl residues or side chains of xylosyl, galactosyl, and fucosyl residues (Zablackis et al., 1995; Liepman et al., 2010). Glucuronoarabinoxylan (4% of the wall) is also found in Arabidopsis leaves (Zablackis et al., 1995). Primary walls of dicotyledonous plants generally also contain 3 to 5% of the hemicelluloses mannan and glucomannan (Scheller and Ulvskov, 2010). Hence, hemicelluloses in primary walls of dicotyledonous plants are mainly composed of Glc, Xyl, Ara, Gal, and Man.

Pectins are a diverse group of polysaccharides that all contain galacturonic acid (GalA) and make up ~50% of Arabidopsis leaf walls (Zablackis et al., 1995; Harholt et al., 2010). Homogalacturonan (HG) is a linear homopolymer of (1,4)-α-linked GalA residues and it makes up ~65% of all pectin in Arabidopsis leaf walls (Zablackis et al., 1995; Mohnen, 2008). A linear (1,4)-α-linked GalA backbone substituted with single xylose residues is called xylogalacturonan, and a polymer with complex side chains containing borate ions and sugars such as Ara, Rha, Gal, Xyl, or Fuc is referred to as rhamnogalacturonan II (Mohnen, 2008; Harholt et al., 2010). Xylogalacturonan and rhamnogalacturonan II make up less than 10% of leaf cell wall pectin (Zandleven et al., 2007; Mohnen, 2008). In contrast, rhamnogalacturonan I backbones consist of a repeating α-1,4-D-GalA-α-1,2-L-Rha disaccharide and are substituted with β-(1,4)-galactan, branched arabinan, or arabinogalactan side chains (Mohnen, 2008; Harholt et al., 2010). RGI constitutes ~20 to 25% of pectin in primary walls (Mohnen, 2008). Hence, pectin in Arabidopsis leaf cell walls consists mostly of GalA, Rha, and smaller amounts of other sugars, including Ara, Gal, Xyl, and Fuc.

In general, carbohydrate biosynthesis requires nucleotide sugars provided by nucleotide sugar interconversion pathways (Seifert, 2004). Most nucleotide sugars are synthesized from UDP-Glc. UDP-glucuronic acid is made from UDP-Glc by UDP-glucose dehydrogenase activity or via an alternative pathway requiring inositol oxygenase activity (Tenhaken and Thulke, 1996; Loewus and Murthy, 2000). UDP-D-glucuronate 4-epimerases (GAEs)

[1] Address correspondence to gbethke@umn.edu.
[2] Current address: University of Louisville, 500 S. Preston Street, Louisville, KY 40202.
The author responsible for distribution of materials integral to the findings presented in this article in accordance with the policy described in the Instructions for Authors (www.plantcell.org) is: Jane Glazebrook (jglazebr@umn.edu).
www.plantcell.org/cgi/doi/10.1105/tpc.15.00404

interconvert UDP-D-GlcA and UDP-D-GalA, the monomeric precursor of pectin. There are six *GAE* genes encoded by the *Arabidopsis* genome. When heterologously expressed in *Escherichia coli* or *Pichia pastori*, GAE1, GAE4, and GAE6 showed activity in interconverting UDP-D-GlcA and UDP-D-GalA (Gu and Bar-Peled, 2004; Mølhøj et al., 2004; Usadel et al., 2004). GAE1 and GAE6 were found to be Golgi localized and strongly expressed in various plant tissues (Mølhøj et al., 2004; Usadel et al., 2004; Parsons et al., 2012). *GAE1* and *GAE6* have been hypothesized to be evolutionarily older than the other *GAE* family members (Usadel et al., 2004) and might have overlapping functions that are distinct from the other family members.

Plant cell wall composition and architecture affects wall strength and flexibility, and cell walls present a physical barrier to potential plant pathogens. Besides preformed physical barriers, such as a cell wall, plants have a sophisticated immune system to defend themselves against harmful microbial pathogens (Chisholm et al., 2006; Jones and Dangl, 2006). Immune signaling involves changes in phytohormone levels, the most important for plant immunity being salicylic acid (SA), jasmonic acid (JA), and ethylene (ET) (Grant and Jones, 2009; Pieterse et al., 2012). Other major regulators of plant immunity include *PHYTOALEXIN DEFICIENT4* (*PAD4*) and *ENHANCED DISEASE SUSCEPTIBILITY1* (*EDS1*) (Wiermer et al., 2005). Immune signaling generally involves changes in the transcriptome that, in turn, lead to altered cellular responses (Tao et al., 2003). For instance, induced expression of the cytochrome P450 *PAD3* is thought to increase production of the antimicrobial secondary metabolite camalexin (Zhou et al., 1999).

Because plant cell walls are important barriers against pathogenic microbes, alterations in wall structural properties can lead to changes in plant immunity. To date, only a few examples of cell wall-related mutants with altered pathogen phenotypes have been studied in detail. Mutants impaired in callose biosynthesis, *powdery mildew resistant4* (*pmr4*), display enhanced resistance to the powdery mildew pathogens *Golovinomyces orontii* and *Golovinomyces cichoracearum* (Nishimura et al., 2003). These plants have constitutively high SA levels, and SA signaling is required for the resistance phenotype (Nishimura et al., 2003). Other plants with enhanced resistance to these powdery mildew pathogens include *pmr5*, a mutant enriched in pectin, and *pmr6*, a mutant with a defect in a pectate lyase-like gene (Vogel et al., 2002, 2004). Plants with mutations in cellulose synthases required for primary and secondary wall formation also show increased resistance to pathogens (Ellis and Turner, 2001; Hernández-Blanco et al., 2007). Enhanced resistance to powdery mildew and *Pseudomonas syringae* pv *maculicola* ES4326 (*Pma* ES4326) in *constitutive expression of VSP 1* (*cev1*), which is mutated in the primary wall cellulose synthase *CesA3*, was linked to constitutive high JA and ET levels in these plants (Ellis and Turner, 2001; Ellis et al., 2002a). Interestingly, *irregular xylem1* (*irx1*), *irx3*, and *irx5* plants, which carry mutations in the secondary wall-associated cellulose synthases *CesA8*, *CesA7*, and *CesA4*, showed enhanced resistance to the necrotrophic pathogens *Plectosphaerella cucumerina*, *Ralstonia solanacearum*, and *Botrytis cinerea* as well as the biotrophic powdery mildew *G. cichoracearum*, whereas growth of *P. cucumerina* and *R. solanacearum* pathogens was unaltered in *pmr5*, *pmr6*, and *cev1* plants (Hernández-Blanco et al., 2007). This enhanced resistance of the *irx* mutants was independent of SA, JA, or ET signaling, but instead involved abscisic acid signaling (Hernández-Blanco et al., 2007). Changes in wall structure are likely monitored by the plants and effects may be counteracted through initiation of defense responses that can lead to altered phytohormone levels.

Although plant cell walls serve as barriers against pathogen entry, many pathogens secrete cell wall-degrading enzymes and thus are able to successfully infect their host plants (Albersheim et al., 1969). For example, the *B. cinerea* polygalacturonase Bc-PG1 is required for full virulence of this pathogen, and the gene encoding it shows evidence for diversifying selection, as would be expected for a virulence gene (ten Have et al., 1998; Rowe and Kliebenstein, 2007). Secretion of cell wall-degrading enzymes can trigger the release of cell wall fragments, which can act as damage-associated molecular patterns that activate plant immune responses (Hahn et al., 1981; Ferrari et al., 2013). Similarly, pectin fragments known as oligogalacturonides (OGs) can trigger plant immune responses (Côté and Hahn, 1994; Ferrari et al., 2013). Such responses include the production of reactive oxygen species (ROS), activation of mitogen-activated protein kinase (MAPK) activation and enhanced expression of defense-related genes such as *PAD3* (Ferrari et al., 2007; Denoux et al., 2008; Galletti et al., 2008; Galletti et al., 2011). Some of these responses require SA, JA and ET, whereas others are independent of these phytohormones (Ferrari et al., 2007).

Here, we describe two *GAE* family members, *GAE1* and *GAE6*, whose expression is repressed upon pathogen challenge. A *gae1 gae6* double mutant has brittle leaves and its walls are reduced in pectin, specifically HG and likely RGI. Resistance to the bacterial pathogen *Pma* ES4326 and the fungal necrotroph *B. cinerea* is compromised in *gae1 gae6*. Callose deposition is reduced in *gae1 gae6* plants after treatment with *B. cinerea* isolate Gallo 1. Furthermore, these plants show altered activation of immune signaling in response to treatment with macerozyme, a polygalacturonase that degrades pectin, and they also are hyperresponsive to JA signaling. Macerozyme treatment released less soluble, likely low molecular weight pectin from isolated *gae1 gae6* cell walls than from Col-0 cell walls. *B. cinerea*-induced accumulation of soluble, likely low molecular weight pectin was also decreased in *gae1 gae6* plants. Additionally, *gae1 gae6* plants are impaired in macerozyme-induced immunity to *B. cinerea*, possibly due to decreased release of OGs from their cell walls.

RESULTS

GAE1 and *GAE6* Expression Is Repressed by *Pma* ES4326-Induced Immune Signaling

Our previous research suggested that the status of pectin, specifically pectin modification by methylesterification, is important for plant immunity against *Pma* ES4326 (Bethke et al., 2014). Here, we investigate whether pectin abundance, in addition to its specific structure, is also important for plant immunity by taking a closer look at the formation of the pectin precursor UDP-GalA by GAEs.

Microarray experiments showed that expression of *GAE1* and *GAE6* was repressed in Arabidopsis plants treated with *Pma* ES4326 (Wang et al., 2008). Repression of *GAE1* and *GAE6* in

wild-type Arabidopsis Col-0 plants treated with *Pma* ES4326 was confirmed by qRT-PCR (Figure 1). To test if this repression is mediated by immune signaling, qRT-PCR was also performed in mutants with blocked immune signaling (Figure 1; Supplemental Figure 1). Generally, immunity to *Pma* ES4326 requires intact SA signaling. Repression of both *GAE1* and *GAE6* required the presence of the major immune regulators *EDS1* and *PAD4*, required for SA signaling as well as other immune responses (Jirage et al., 1999; Wiermer et al., 2005; Bartsch et al., 2006; Wang et al., 2008) at both early and late time points. The presence of *AVRPPHB SUSCEPTIBLE3* (*PBS3*), a regulator of many immune responses including SA signaling, (Nobuta et al., 2007), was also required for repression of *GAE1* and *GAE6* at an early time point (Figure 1). *CALMODULIN BINDING PROTEIN 60-LIKE a* (*CBP60a*) (a negative regulator of SA synthesis and immunity; Truman et al., 2013), *CBP60g*, *SYSTEMIC ACQUIRED RESISTANCE DEFICIENT1* (*SARD1*) (both promote SA biosynthesis and regulation of other immune responses; Wang et al., 2011), *SALICYLIC ACID INDUCTION DEFICIENT2* (*SID2*) encodes a biosynthetic enzyme for SA; Wildermuth et al., 2001), and *NONEXPRESSER OF PR GENES1* (a regulator of the majority of SA-induced immune signaling; Cao et al., 1997; Yan and Dong, 2014) were not required for this repression (Figure 1; Supplemental Figure 1). Thus, repression of *GAE1* and *GAE6* requires a regulatory function that is dependent on *EDS1* and *PAD4*, partially dependent on *PBS3*, but independent of SA.

There are six *GAE* family members in Arabidopsis. *GAE2* expression was induced by *Pma* ES4326 in the absence of *PAD4* or *EDS1*, *GAE3* expression was unaltered, *GAE4* was repressed early, and *GAE5* expression was induced in all genotypes (Supplemental Figure 2). The similarity of the immune-regulated expression of *GAE1* and *GAE6* suggested a redundant role of these genes in Arabidopsis immunity to *Pma* ES4326.

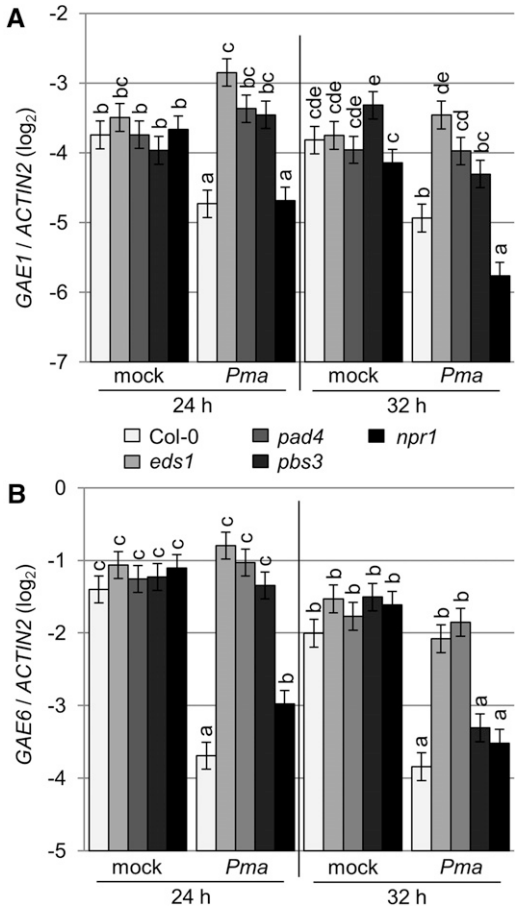

Figure 1. *Pma* ES4326-Induced Repression of *GAE1* and *GAE6* Expression Requires *PAD4*, *EDS1*, and *PBS3*.

(A) Expression of *GAE1* in leaves of wild-type Col-0 and mutant plants. Expression was measured 24 or 32 h after either inoculation with *Pma* ES4326 (OD_{600} = 0.002) or mock inoculation with 5 mM $MgSO_4$ and was then normalized to the level of *ACTIN2*. Data from three biological replicates were combined using a mixed linear model. Bars represent mean $\log_2$ ratios to *ACTIN2* ± SE. Letters indicate significantly different groups with $q < 0.05$, where 0.05 represents the maximum false discovery rate at which the test may be called significant.
(B) Expression of *GAE6* measured as described in **(A)**.

Resistance to *Pma* ES4326 Is Compromised in *gae1 gae6* and *gae6* Plants

To study the roles of *GAE1* and *GAE6* in plant immunity in more detail, plants with T-DNA insertion mutations in *GAE1* and *GAE6* were obtained from the SALK collection as described in the Accession Numbers section in Methods. We identified two *GAE6* knockout alleles, *gae6-1 and gae6-2*, and a T-DNA insertion in *GAE1*, *gae1-1*, that caused reduced expression of this gene (Supplemental Figure 3). A double mutant was created by crossing *gae1-1* and *gae6-1*. Both *gae6* and *gae1 gae6* plants were more susceptible to *Pma* ES4326 than wild-type Col-0 and *gae1* plants, supporting a role of *GAE6* in plant immunity to *Pma* ES4326 (Figure 2).

gae6 and *gae1 gae6* Plants Have Brittle Leaves

While inoculating leaves of *gae1 gae6* plants, we noticed that the petioles and midribs of these plants tended to break easily when leaves were bent against the proximal-distal axis of the leaves (Figure 3; Supplemental Figures 4D to 4F). They tended to break less often when twisted around the proximal-distal axis. To quantify this phenotype, leaves were bent by 180° (Figure 3A) and breaking of midribs or petioles was recorded. Most *gae1 gae6* leaves broke, whereas fewer leaves of *gae6* plants and very few leaves of wild-type Col-0 and *gae1* plants did (Figure 3B; Supplemental Figure 4C). Although *gae1 gae6* plants had slightly shorter leaves and petioles than wild-type plants (Supplemental Figures 4A and 4B), no correlation between leaf size or petiole length and breaking frequency was detected. We also investigated tissue integrity by monitoring ion leakage. Interestingly, when leaves were inoculated with deionized water, leaf discs of *gae1 gae6* leaked more ions than wild-type Col-0 discs (Figure 3C), suggesting that the increased brittleness is correlated with a structural defect that promotes increased ion leakage. Taken together, these results showed that loss of *GAE6* causes brittle leaves and additional loss of *GAE1* strongly enhances this phenotype. We conclude that *GAE1* and *GAE6* contribute to normal leaf flexibility.

Cell Walls of *gae6* and *gae1 gae6* Plants Have Lower Levels of Pectin

GalA is a major component of pectin. We analyzed wall monosaccharide composition in *gae* mutants to investigate whether the increased brittleness was associated with an altered wall composition of *gae* leaves. To approximate pectin content of *gae* mutant walls, the total uronic acid concentration was measured using a simple colorimetric assay (Filisetti-Cozzi and Carpita, 1991; van den Hoogen et al., 1998). Total uronic acid was reduced in *gae6-2* and strongly reduced in *gae1 gae6* plants but was indistinguishable from wild-type Col-0 in *gae6-1* and *gae1* (Supplemental Figure 5). This suggested that *gae1 gae6* and possibly *gae6* plants have reduced pectin.

To investigate the cell wall composition in leaves of *gae* plants in more detail, we measured the levels of seven neutral monosaccharides, the acidic sugars GalA (the monomeric subunit of the pectin backbone; Harholt et al., 2010) and GlcA (Figure 4). We also estimated the crystalline cellulose content (Updegraff, 1969). Cell walls of both *gae6* mutants and *gae1 gae6* were reduced in GalA (Figure 4A). In *gae1 gae6*, GalA content in cell walls was reduced by more than 40% compared with the wild-type level. GlcA levels were indistinguishable between mutants and the wild type (Figure 4B). Cellulose content was higher in *gae6-2* and *gae1 gae6* walls, likely due to the loss of pectins (Figure 4C). Cell walls of *gae1 gae6* plants were also enriched in all neutral sugars measured, presumably due to the substantial proportional loss of GalA (Figure 4D). The levels of most wall monosaccharides were even higher in the *gae1 gae6* double mutant with the exception of Rha, which did not exhibit a significant increase compared with the *gae6* single mutants. The absence of a compensational increase in Rha suggested that RGI, the dominant Rha contributor to the wall, may be considered reduced in *gae1 gae6* mutants compared with the wild type albeit not to such an extent as HG.

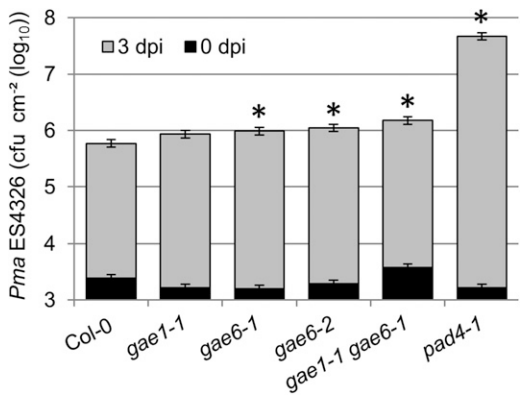

Figure 2. Susceptibility of *gae6* and *gae1 gae6* Plants to *Pma* ES4326 Is Increased Relative to Wild-Type Col-0.

Leaves of plants of the indicated genotypes were inoculated with *Pma* ES4326 (OD_{600} = 0.0002) as described in Methods. Bacterial titers in leaves were determined either immediately (0 dpi) or after 3 d (3 dpi). Bars represent the mean ± SE of four independent experiments, each with 4 or 12 biological replicates at 0 and 3 dpi, respectively. Data were combined using a mixed linear model. Asterisks indicate significant differences from Col-0 wild type ($q < 0.05$). Susceptible *pad4* plants were included as a positive control. cfu, colony-forming units.

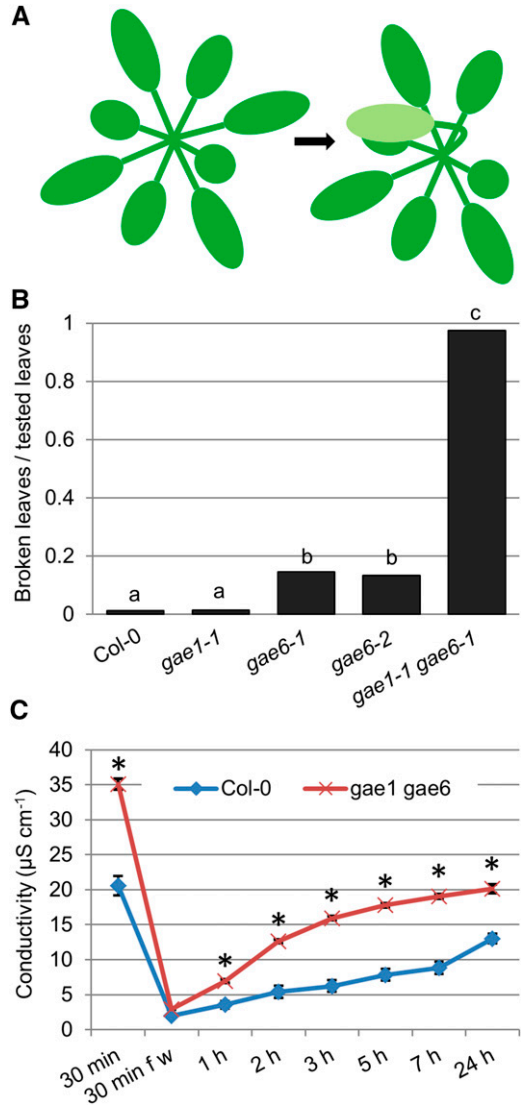

Figure 3. Mutant *gae6* and *gae1 gae6* Plants Have Brittle Leaves.

(A) Depiction of the assay for brittleness of *gae* mutant leaves. Fully expanded leaves of 4- to 5-week-old plants were bent by 180° so that the adaxial surface of the leaf was parallel with the soil. Broken leaf petioles or midribs were considered brittle.

(B) Quantification of broken midribs or petioles. For each genotype, 66 to 82 leaves were analyzed for brittleness as described in **(A)**. Bars represent the ratio of broken to total number of leaves tested. Results were analyzed using Fisher's exact test. Letters indicate significantly different groups at $P < 0.05$.

(C) Conductivity measurements. Leaves of 4-week-old plants were inoculated with deionized water and then leaf discs were cut out and placed on deionized water. Conductivity was measured at the indicated time points. After 30 min, the water was replaced with fresh water (30 min fresh weight) to account for wounding-related ion leakage from the edges of the leaf discs. Three independent experiments with six biological replicates each were performed and data were analyzed using a *t* test for each time point. P values were corrected using the Bonferroni method. Data show means ± SE; asterisks indicate significant differences from wild-type Col-0 at $q < 0.01$.

To further investigate which pectic components were altered in *gae1 gae6*, dot blot experiments using pectin isolated from the various genotypes were performed. Both LM19 and LM20 antibodies recognize HG (Verhertbruggen et al., 2009a). As expected, LM19 binding was reduced in *gae6-1* and *gae1 gae6* (Figures 5A and 5B) and LM20 binding was reduced in *gae1 gae6* (Figures 5C and 5D). This result confirmed that *gae1 gae6* cell walls are reduced in HG. Using the same samples, we detected no difference from the wild type in binding of LM5, which recognizes a tetramer of (1-4)-β-D-galactans found in RGI (Jones et al., 1997), LM6, which recognizes a linear pentasaccharide in (1-5)-α-L-arabinans found in RGI (Willats et al., 1998; Verhertbruggen et al., 2009b), LM8, which recognizes xylogalacturonan (Willats et al., 2004), or CCRC-M7, which recognizes an arabinosylated (1-6)-β-D-galactan epitope occurring on RGI (Puhlmann et al., 1994; Steffan et al., 1995; Pattathil et al., 2010) (Supplemental Figure 6). Collectively, these cell wall composition data show that *gae1 gae6* plants are reduced in HG. Due to the strong proportional reduction of HG in the walls, levels of all other components should be higher. However, Rha indicative of RGI was not higher in *gae1 gae6*, suggesting that RGI may also be reduced in *gae1 gae6* walls.

GAE1 and *GAE6* Are Required for Immunity to Specific *B. cinerea* Isolates

We hypothesized that plant immunity to *B. cinerea* might be affected by pectin content in the host cell wall because this pathogen requires polygalacturonases and pectin methylesterases for full virulence (ten Have et al., 1998; Valette-Collet et al., 2003; Kars et al., 2005b; Espino et al., 2010). Because *B. cinerea* is genetically diverse and has a high diversity of polygalacturonases (Rowe and Kliebenstein, 2007), we measured relative fungal growth at both 2 and 3 d postinoculation (dpi) using 10 different *B. cinerea* isolates (Figure 6). The *B. cinerea* isolates Fresa 525 and Gallo 1 showed enhanced virulence on *gae1 gae6* plants at both time points, whereas KT and UK Razz showed enhanced virulence in *gae1 gae6* plants at 3 but not 2 dpi (Figure 6A). We did not detect any significant changes in relative fungal growth between wild-type Col-0 and *gae1 gae6* plants when using Acacia, Apple 517, DN, Grape, Pepper, or Rasp isolates of *B. cinerea*. Therefore, we continued our study using Gallo 1 and Fresa 525. We also included Pepper for comparison, as this isolate has been used in a large-scale analysis of plant gene expression in response to *B. cinerea* infection (Windram et al., 2012).

We next investigated whether expression of *GAE1* and *GAE6* was affected by challenge with *B. cinerea*. Inoculation of wild-type Col-0 plants with any isolate repressed *GAE1* and *GAE6* expression (Figures 6B and 6C), and this repression was generally independent of *PAD4* (Figures 6B and 6C). Expression of *GAE2* and *GAE3* was unaltered by *B. cinerea* treatment. *GAE4* was repressed only by Fresa 525 treatment, while *GAE5* expression was enhanced with all three isolates tested (Supplemental Figure 7). As seen for infection with *Pma* ES4326, the expression of *GAE1* and *GAE6* was repressed upon *B. cinerea* treatment. This indicates a role for *GAE1* and *GAE6* in the immune response to *B. cinerea*.

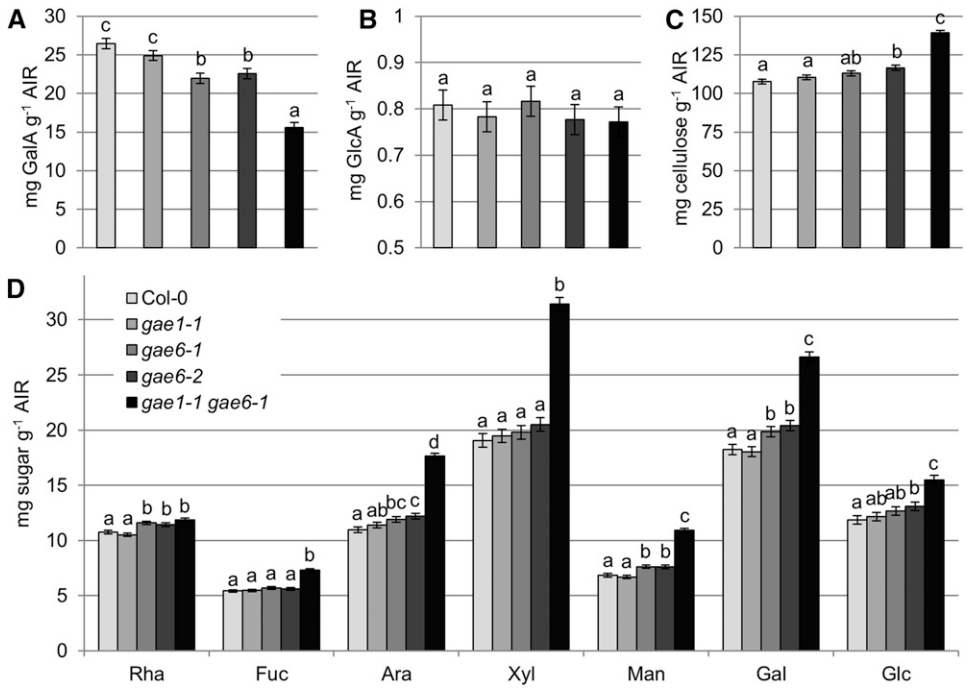

Figure 4. Cell Walls of *gae6* and *gae1 gae6* Plants Are Reduced in GalA.

Levels of GalA **(A)**, GlcA **(B)**, cellulose **(C)**, and neutral sugars **(D)** in AIR extracted from leaves of 4-week-old plants of the indicated genotypes. Bars represent means ± SE of four biological replicates combined using a mixed linear model. Letters indicate significantly different groups ($P < 0.05$).

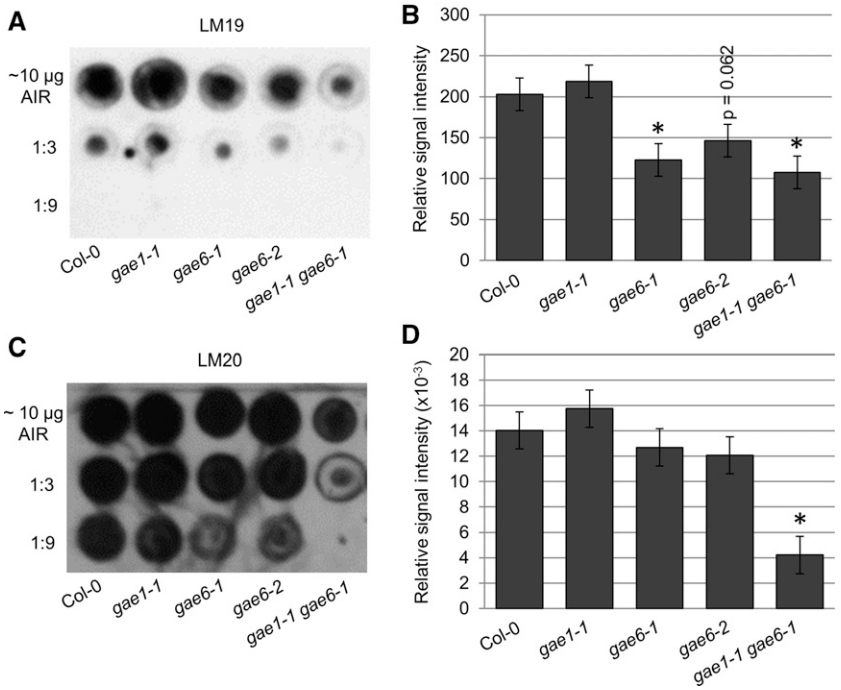

Figure 5. Cell Walls of *gae1 gae6* Plants Are Reduced in Homogalacturonan.

Dot blot analyses with anti-LM19 and anti-LM20 antibodies. Pectin was extracted from AIR prepared from the indicated genotypes using 1 μL of extraction buffer per 10 μg of AIR. Pectin was serially diluted and 1 μL of undiluted, 1:3 diluted, and 1:9 diluted samples were spotted on a nitrocellulose membrane. Three biological replicates were spotted twice to obtain two technical replicates each. All replicates produced similar results. Relative signal intensities were measured using Image J software. Measurements from the three biological replicates were combined using a linear model after Box-Cox power transformation as described in Methods. Bars represent means ± SE. Asterisks indicate a difference from wild-type Col-0 at $P < 0.05$.

(A) Representative dot blot using anti-LM19 antibody.

(B) Relative signal intensities of the spots in the dot blot in **(A)**.

(C) Representative dot blot using anti-LM20 antibody.

(D) Relative signal intensities of the LM20 dot blot shown in **(C)**.

Pectinase-Induced Immune Signaling Is Altered in *gae1 gae6* Plants

Because the amount of pectin substrate for pathogen polygalacturonases is reduced, we hypothesized that immunity phenotypes of *gae1 gae6* plants may result from reduced generation of OGs by these enzymes. In turn, the reduced OGs could lead to reduced immune responses. To test this, we used macerozyme, a commercial pectinase, as a proxy for pathogen pectinases. We isolated cell walls as a subcellular fraction known as alcohol-insoluble residue (AIR; Gille et al., 2009). This was treated with macerozyme and tested for release of soluble, likely low molecular weight, pectin fragments (Figure 7). Treatment with 0.25% macerozyme released significantly more uronic acid from wild-type Col-0 AIR relative to *gae1 gae6* AIR (Figure 7B). To test activity of these pectin-containing solutions, we infiltrated them into wild-type Col-0 plants and measured *PAD3* expression. *PAD3* is required for synthesis of the phytoalexin camalexin (Zhou et al., 1999) and its expression is known to be induced by OG treatment (Ferrari et al., 2007). Fractions from macerozyme-treated Col-0 walls induced significantly more *PAD3* expression than fractions derived from *gae1 gae6* walls, suggesting that macerozyme treatment did indeed release more active soluble uronic acid, possibly OGs, from wild-type Col-0 walls than from *gae1 gae6* walls (Figure 7C).

Next, we studied the effect of macerozyme treatment on expression of *PAD3* in intact plants (Figure 8). This treatment did not lead to any visible leaf damage (Supplemental Figure 8). In wild-type Col-0, *PAD3* expression was induced three h after treatment with 0.01% macerozyme (Figure 8A). By contrast, no macerozyme-induced induction of *PAD3* expression was detected in *gae1 gae6* (Figure 8A). However, OG treatment induced the expression of *PAD3* in both genotypes, indicating that *gae1 gae6* plants do respond to OGs (Figure 8B). Macerozyme treatment also induced expression of the SA marker genes *PATHOGENESIS RELATED1* (*PR1*) and *SID2* in Col-0, but not in *gae1 gae6* (Figures 9A and 9B). *PR1* was not significantly induced by purified OGs (Figure 9C) at the time and concentration tested, but *SID2* was induced by OG treatment in both genotypes (Figure 9D). However, the induction was stronger in wild-type Col-0. In addition, the JA markers *JASMONATE-ZIM-DOMAIN PROTEIN5* (*JAZ5*) and *JAZ10* were induced by macerozyme and OG treatment in both Col-0 and *gae1 gae6* (Figure 10A; Supplemental Figure 11). Interestingly, expression of *JAZ5* and *JAZ10* was already strongly

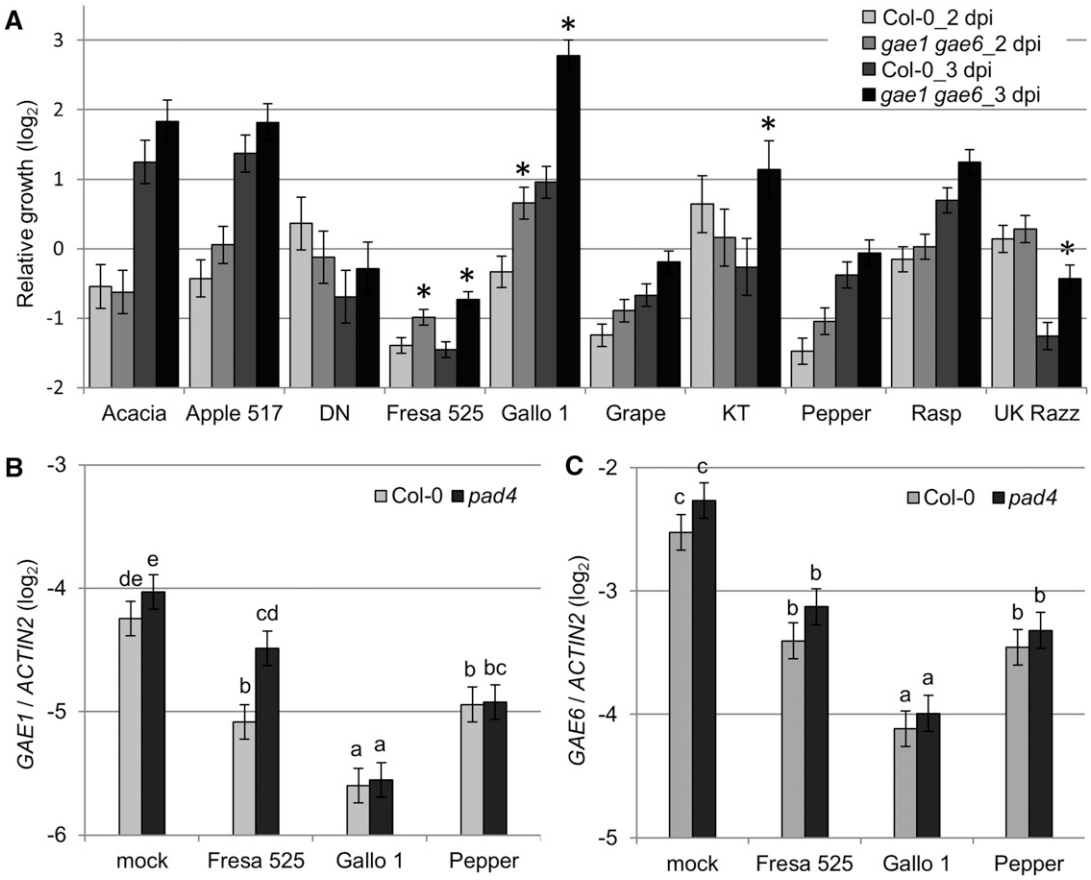

Figure 6. Growth of *B. cinerea* on *gae1 gae6* Plants and the Effect of *B. cinerea* on Expression of *GAE1* and *GAE6*.

(A) Growth of *B. cinerea* isolates. Leaves of Col-0 and *gae1 gae6* plants were inoculated with 2.5×10^5 spores mL^{-1} of the *B. cinerea* isolates indicated in the figure. Samples were collected two (2 dpi) and three (3 dpi) days later. Bars represent means ± SE of six biological replicates for each fungus, combined using a mixed linear model. Asterisks indicate significant differences from wild-type Col-0 for each isolate ($P < 0.05$).
(B) and **(C)** Expression of *GAE1* **(B)** and *GAE6* **(C)** 48 h after inoculation with the *B. cinerea* isolates indicated. Expression levels were measured by qRT-PCR. Bars represent mean $\log_2$ ratios to *ACTIN2* ± SE of three biological replicates, combined using a mixed linear model. Letters indicate significantly different groups ($q < 0.05$).

induced in *gae1 gae6* after mock inoculation (Figure 10; Supplemental Figure 11). We observed no hyperresponsive induction by mock treatment of *PLANT DEFENSIN 1.2* (*PDF1.2*), a necrotrophy and late JA signaling marker gene (Supplemental Figures 12A to 12D). *PDF1.2* was also not induced by macerozyme or OG treatments (Supplemental Figures 12A to 12D). This suggests that early JA signaling is induced by mock treatment in *gae1 gae6*. Because it is known that JA and SA signaling act antagonistically (Pieterse et al., 2012), the strong upregulation of JA-induced immune signaling in *gae1 gae6* might explain the lower OG-induced *SID2* expression in this genotype.

To test whether other immune responses are altered in *gae1 gae6* plants, we analyzed mitogen-activated protein kinase (MAPK) activity following macerozyme and OG treatments. OGs are known to activate the MAPKs MPK3 and MPK6 in Arabidopsis (Galletti et al., 2011). Macerozyme treatment activated MPK3 and MPK6 in wild-type Col-0, whereas MAPK activation in *gae1 gae6* was slightly reduced in four out of five experiments performed (Supplemental Figure 13). By contrast, OG-induced MAPK activity was similar or increased in *gae1 gae6* in four out of five experiments (Supplemental Figure 13). Additionally, mock treatment induced MAPK activity in *gae1 gae6* more strongly than it did in wild-type Col-0 in four out of five experiments performed (Supplemental Figure 13). Collectively, these results illustrate that activation of several immune signaling components—camalexin synthesis, SA and JA signaling, and possibly MAPK activation—by macerozyme is substantially altered in *gae1 gae6*. This suggests that release of soluble pectin fragments, possibly OGs, by pectinolytic enzymes might be reduced in *gae1 gae6* plants while recognition of OGs is intact.

Following *B. cinerea* Infection, Production of Soluble Pectin and Deposition of Callose Are Reduced in *gae1 gae6* Plants

Although *pad3* plants were more susceptible to the *B. cinerea* isolates Fresa 525 and Gallo 1, which also grew better on *gae1*

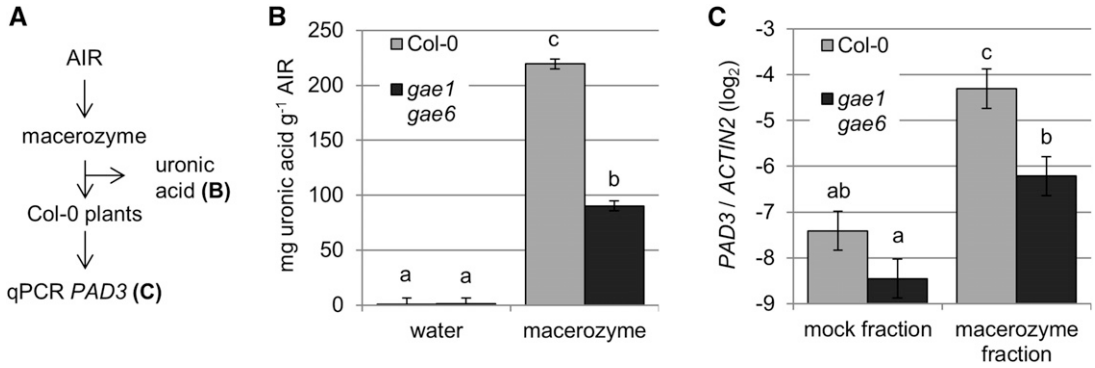

Figure 7. Levels of Soluble Pectin and Expression of *PAD3* in Fractions Produced Following Macerozyme Treatment of *gae1 gae6* Cell Walls.

(A) Schematic overview of the experimental procedure for **(B)** and **(C)**.

(B) Uronic acid measurements. AIR from leave tissue of 4-week-old wild-type Col-0 or *gae1 gae6* plants was treated with water or 0.25% macerozyme and assayed for uronic acid levels. Data from 11 biological replicates were combined using a mixed linear model. Bars represent means ± SE. Letters indicate significant differences ($P < 0.05$).

(C) Expression of *PAD3* in Col-0 plants treated with the fractions from **(B)**. Extracts from **(B)** were heat inactivated, pooled, and diluted 5-fold with water. Pooled extracts were inoculated into 4-week-old Col-0 plants. *PAD3* expression was measured 3 h after inoculation and normalized to the level of *ACTIN2* expression. Data from four biological replicates were combined using a mixed linear model. Bars represent mean $\log_2$ ratios to *ACTIN2* ± SE. Letters indicate significant differences ($P < 0.05$).

gae6, growth of the isolate Pepper was similar on Col-0 and *pad3* (Supplemental Figure 9A). However, we did not detect any significant changes in camalexin production after treatment with *B. cinerea* isolate Gallo 1 and Fresa 525 in *gae1 gae6* (Figure 8D). Neither did we detect changes in *PAD3* expression after treatment with any *B. cinerea* isolate in *gae1 gae6* (Figure 8E). Additionally, *SID2* and *PR1* were similarly induced by all *B. cinerea* isolates in both Col-0 and *gae1 gae6* (Figure 9E and F) and *sid2* plants, which are deficient for pathogen-induced SA biosynthesis, did not show any differences in relative *B. cinerea* growth (Supplemental Figure 9B). Expression of *JAZ10* was induced more strongly by Gallo 1 treatment in *gae1 gae6* than in wild-type Col-0 but not by Fresa 525 or Pepper (Figure 10C), while *dde2* plants, deficient for JA biosynthesis, showed enhanced susceptibility to all *B. cinerea* isolates tested (Supplemental Figure 9B). Curiously, exogenous application of methyl jasmonate (MeJA) did not lead to altered relative fungal growth of *B. cinerea* (Supplemental Figure 9C), and *cev1/isoxaben resistant1* (*ixr1*) plants, which have constitutively high JA levels (Ellis and Turner, 2001), did not show any changes in susceptibility to the *B. cinerea* isolates tested (Supplemental Figure 9D). Hence, neither differences in *B. cinerea* isolate susceptibility to camalexin nor altered SA or JA signaling by themselves explained the enhanced susceptibility of *gae1 gae6* to these *B. cinerea* isolates.

Hydrogen peroxide accumulation in response to *B. cinerea* isolates Fresa 525, Gallo 1, and Pepper was not obviously altered in *gae1 gae6* plants (Supplemental Figure 14). However, callose deposition upon treatment with *B. cinerea* isolate Gallo 1 was strongly reduced in *gae1 gae6* (Figure 11). It was previously shown that OG treatment induces callose deposition (Denoux et al., 2008), suggesting that the reduction in callose deposition might be due to reduced OG release in *gae1 gae6*. It is possible that this reduction in callose deposition contributes to the reduced immunity of *gae1 gae6* plants to *B. cinerea* isolate Gallo 1.

Because macerozyme could be used to release soluble, likely low molecular weight pectin from isolated cell walls, we next investigated whether infection with *B. cinerea* was accompanied by accumulation of soluble pectin as well. We prepared cell walls (AIR fraction) from leaves infected with *B. cinerea*, incubated these cell walls with water, and measured uronic acid content of the extracts. *B. cinerea* treatment did in fact lead to increased accumulation of soluble pectin in wild-type Col-0 plants when compared with mock-treated samples (Figure 12). No such increased accumulation of water-soluble pectin fractions was observed in *gae1 gae6* (Figure 12).

Macerozyme-Induced Pattern-Triggered Immunity against *B. cinerea* Is Abolished in *gae1 gae6*

It was previously shown that OG treatment can induce pattern-triggered immunity (PTI) to *B. cinerea* (Ferrari et al., 2007). We tested macerozyme treatment to determine whether it could also induce PTI to the *B. cinerea* isolate Gallo 1 (Figure 13). Indeed, pretreatment with 0.01% macerozyme for 24 h led to reduced *B. cinerea* growth in wild-type Col-0 but not *gae1 gae6* plants (Figure 13A). Interestingly, mock and macerozyme pretreated *gae1 gae6* plants exhibited similar growth of *B. cinerea* Gallo 1 as did macerozyme-treated Col-0 plants. This result is likely due to activation of JA signaling in *gae1 gae6* during the pretreatment procedure (Figures 13C and 13D). OG-induced PTI was observed in both genotypes when using a high dose of OGs (Figure 13B), whereas a lower dose of OGs only induced PTI in Col-0 (Supplemental Figure 15). This suggests that OG perception in *gae1 gae6*, at least above a certain threshold, is unaltered, while release of immunity-activating pectin fragments, possibly OGs, is reduced. We conclude that immune responses induced by macerozyme treatment, which do not occur in *gae1 gae6* plants, are important for plant immunity to the *B. cinerea* isolate Gallo 1.

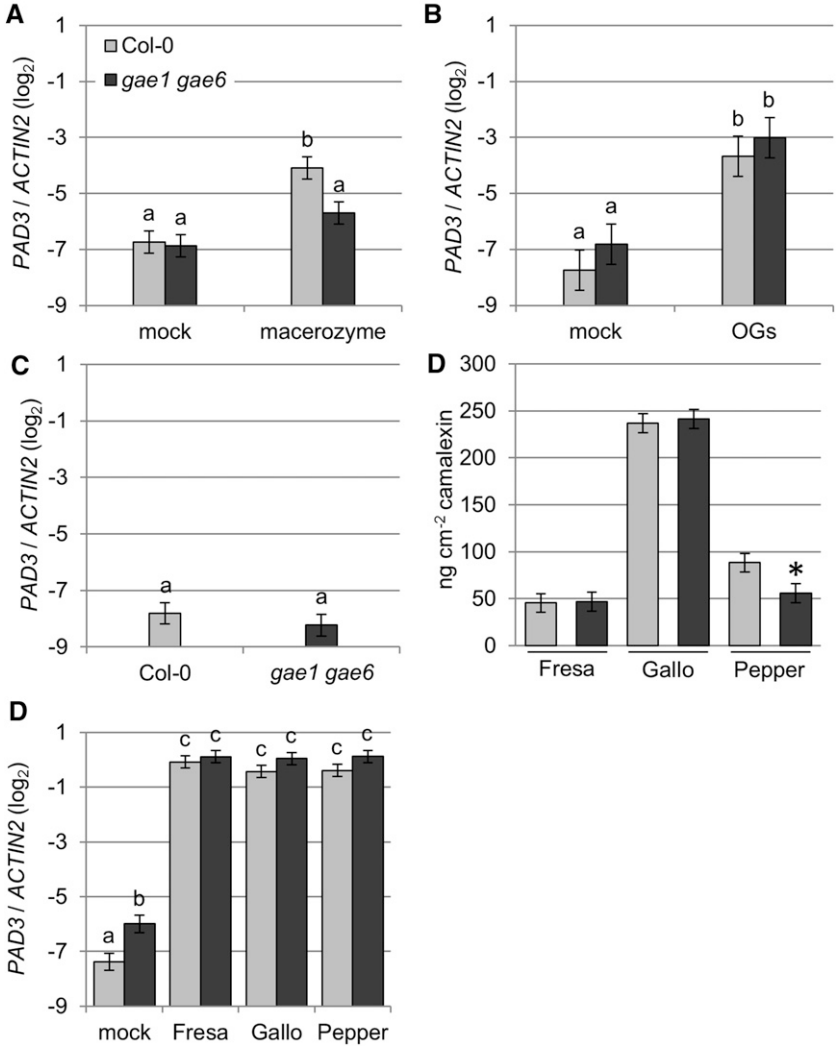

Figure 8. Macerozyme-Induced *PAD3* Expression Is Absent in *gae1 gae6*.

(A) Expression of *PAD3* after macerozyme treatment. Four-week-old plants were either inoculated with 0.01% macerozyme or mock inoculated with water, and *PAD3* expression was measured 3 h later by qRT-PCR. Data from four biological replicates were combined using a mixed linear model. Mean $\log_2$ ratios to *ACTIN2* ± SE were plotted. Letters indicate significantly different groups ($P < 0.05$).

(B) Expression of *PAD3* after OG treatment. *PAD3* expression was measured as described in **(A)** 3 h after inoculation with 100 µg mL^{-1} OGs or mock inoculation with water. Data are from six biological replicates.

(C) *PAD3* expression in untreated plants. Three biological replicates were performed and data analyzed as described in **(A)**.

(D) Camalexin accumulation after *B. cinerea* treatment. Camalexin accumulation was measured in 4-week-old plants inoculated with the *B. cinerea* strains shown in the figure. Eight biological replicates each were combined using a mixed linear model. Asterisks indicate significant differences from wild-type Col-0 for each isolate ($P < 0.05$).

(E) *PAD3* expression 28 h after treatment with the indicated *B. cinerea* strains. Data from six biological replicates were collected and analyzed as described in **(A)**. Data in all figure parts represent means ± SE. Letters indicate significantly different groups ($q < 0.05$).

DISCUSSION

Here, we showed that loss of *GAE1* and *GAE6* leads to a dramatic reduction in pectin content in the cell wall (Figure 4), likely causing the brittleness of leaves that we observed (Figure 3). Petioles and midribs of *gae1 gae6* plants broke easily when bent, and inoculation of leaves with deionized water resulted in increased ion leakage, possibly due either to microscopic fractures of the cell wall induced by inoculation stress or to a reduced capability of these walls to withstand increased turgor pressure. The increased brittleness was associated with altered cell wall composition. In our analysis, the GalA content of *gae1 gae6* leaf walls was reduced by more than 40% and the total uronic acids by over 60% (Figure 4; Supplemental Figure 5). This is a major change in the overall cell wall composition, considering that pectin makes up ~50% of the plant cell walls found in Arabidopsis leaves (Zablackis et al., 1995;

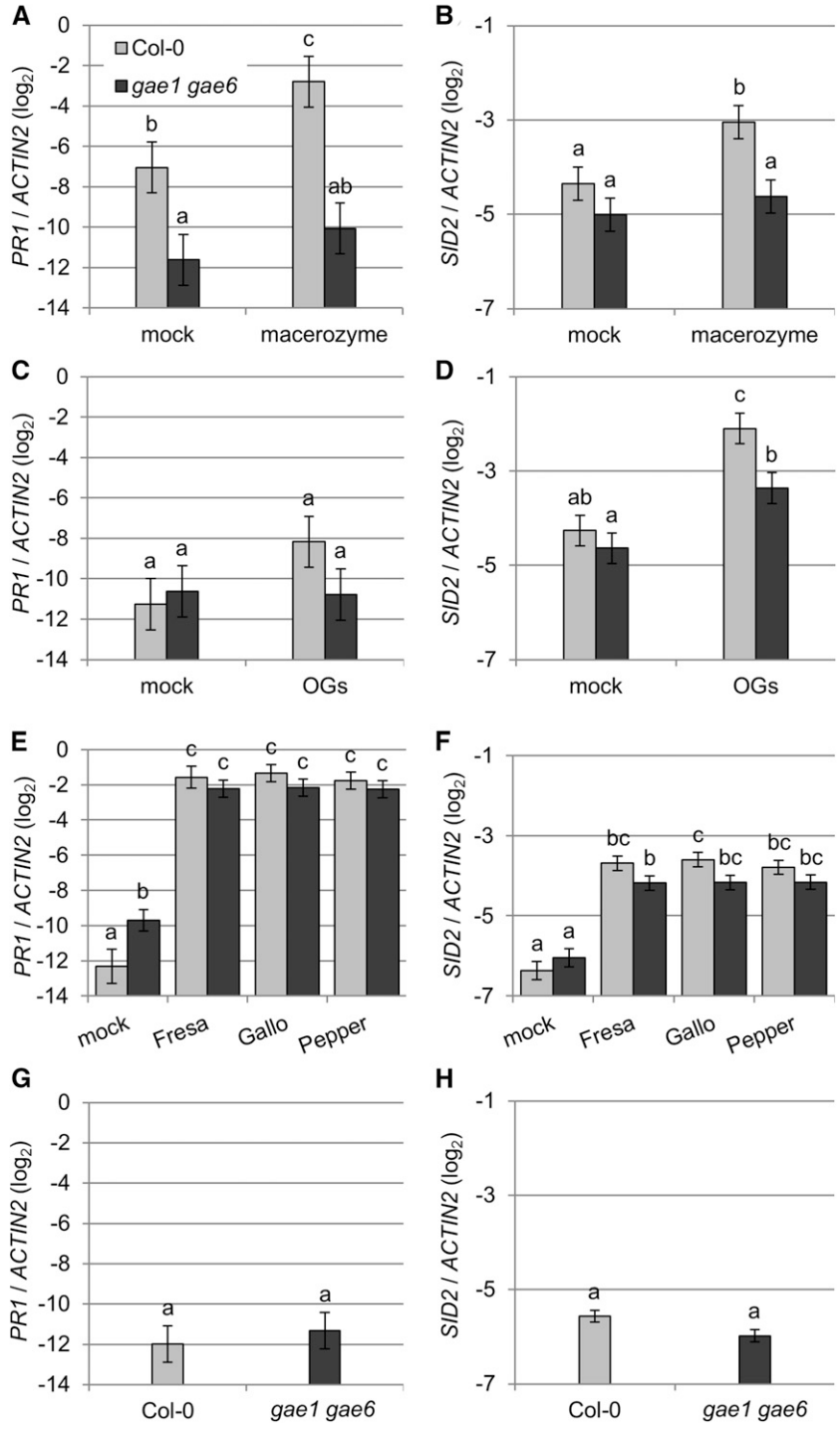

Figure 9. Macerozyme-Induced Expression of the SA Marker Genes *SID2* and *PR1* Is Abolished in *gae1 gae6* Plants.

(A) to **(H)** Expression of *PR1* (**[A]**, **[C]**, **[E]**, and **[G]**) or *SID2* (**[B]**, **[D]**, **[F]**, and **[H]**) in 4-week-old Col-0 and *gae1 gae6* plants. Data were combined using a mixed linear model. Bars represent mean $\log_2$ ratios of expression versus *ACTIN2* ± SE for all figure parts. Letters indicate significantly different groups at $P < 0.05$ for **(A)** to **(D)**, **(G)**, and **(H)** and $q < 0.05$ for **(E)** and **(F)**.

(A) and **(B)** Plants were treated with 0.01% macerozyme or mock treated with water and samples were collected 3 h later. Data from four biological replicates are shown.

(C) and **(D)** Plants were inoculated with 100 µg mL^{-1} OGs or mock treated with water and samples collected 3 h later. Data from six biological replicates are shown.

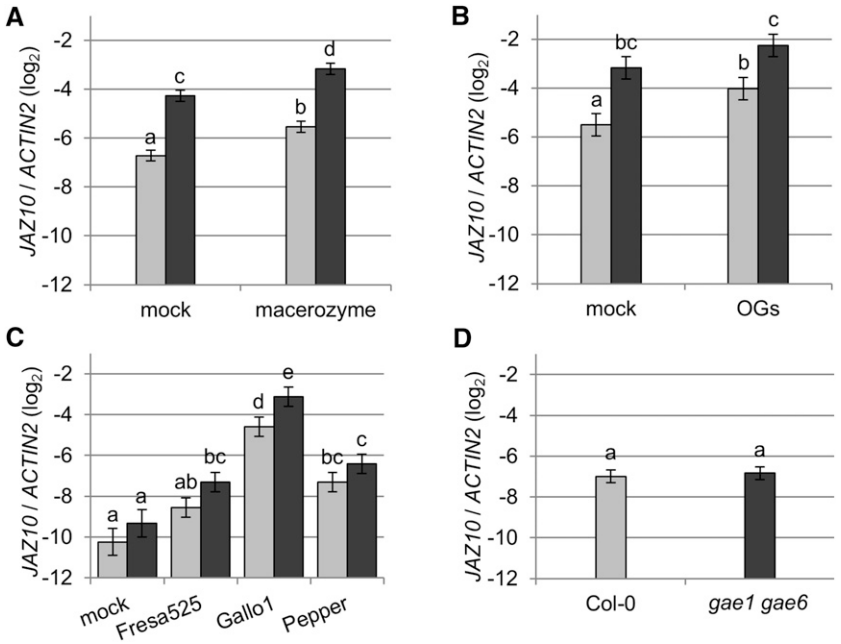

Figure 10. The Expression of the JA Marker Gene *JAZ10* is Highly Responsive in *gae1 gae6* Plants.

(A) to **(D)** *JAZ10* expression in 4-week-old plants. Data were combined using a mixed linear model. Mean $\log_2$ ratios to *ACTIN2* ± SE are shown. Letters indicate significantly different groups at $P < 0.05$ for **(A)**, **(B)**, and **(D)** and $q < 0.05$ for **(C)**.

(A) Plants were inoculated with 0.01% macerozyme or mock inoculated using water and samples were collected 3 h later. Data from four biological replicates are shown.

(B) Plants were inoculated with 100 µg mL^{-1} OGs or mock inoculated using water and samples collected 3 h later. Data are from six biological replicates.

(C) *JAZ10* expression 48 h after treatment with the indicated *B. cinerea* strains. Data are from six biological replicates.

(D) *JAZ10* expression in untreated plants. Data are from three biological replicates.

Nobuta et al., 2007; Harholt et al., 2010). Interestingly, *quasimodo1* (*qua1*) plants, which have a mutation in a glycosyltransferase family 8 gene, are reduced in GalA by 25% and show reduced binding of HG-specific antibodies (Bouton et al., 2002).

Furthermore, *qua2* plants, which have a mutation in a putative methyltransferase, have ~13% less total GalA and lack 50% of cell wall HG (Mouille et al., 2007). Likewise, *cgr2 cgr3* plants, carrying mutations in another class of Golgi-localized putative methyl-transferases, have leaf cell walls that are reduced by ~40% in uronic acid (Kim et al., 2015). All three mutants are severely dwarfed (Bouton et al., 2002; Mouille et al., 2007; Kim et al., 2015). Additionally, *qua1* and *qua2* mutants show a distorted overall shape, likely due to reduced cell cohesion, and are extremely fragile (Bouton et al., 2002; Mouille et al., 2007). By contrast, *gae1 gae6* plants with a similar strong reduction in GalA and total uronic acids have an overall normal shape and are only slightly smaller than wild-type Col-0 (Supplemental Figure 4). In the wall analysis performed here, we did not detect changes in other wall polysaccharides or structures that might compensate for the reduction of pectin in *gae1 gae6*. It is possible the severe morphological alterations in *qua2* and *cgr2 cgr3* plants are due to reduction in pectin methylesterification, which is unaffected in *gae1 gae6*. It was speculated that quality control mechanisms in the Golgi prevent secretion of inefficiently esterified pectin in *cgr2 cgr3* (Kim et al., 2015), suggesting that the Golgi of these plants might overaccumulate pectin and that this may contribute to the severe dwarf phenotype of these plants. The *gae1 gae6* plants described here provide an opportunity to study the effects of reduction of pectin in plants that do not show severe morphological phenotypes.

We found that *gae1 gae6* plants are also compromised in resistance to *B. cinerea* and *Pma* ES4326, indicating that loss of pectin reduces immunity to these pathogens (Figures 2 and 6). We found that *gae1 gae6* plants were slightly more susceptible to *Pma* ES4326 but showed a strong increase in susceptibility to specific *B. cinerea* isolates. This was not unexpected because *B. cinerea* is

Figure 9. (continued).

(E) and **(F)** Plants were inoculated with the indicated *B. cinerea* isolates or mock inoculated with *B. cinerea* inoculation medium and samples collected 48 h later. Data from eight biological replicates are shown.

(G) and **(H)** Expression in untreated plants. Three biological replicates were performed.

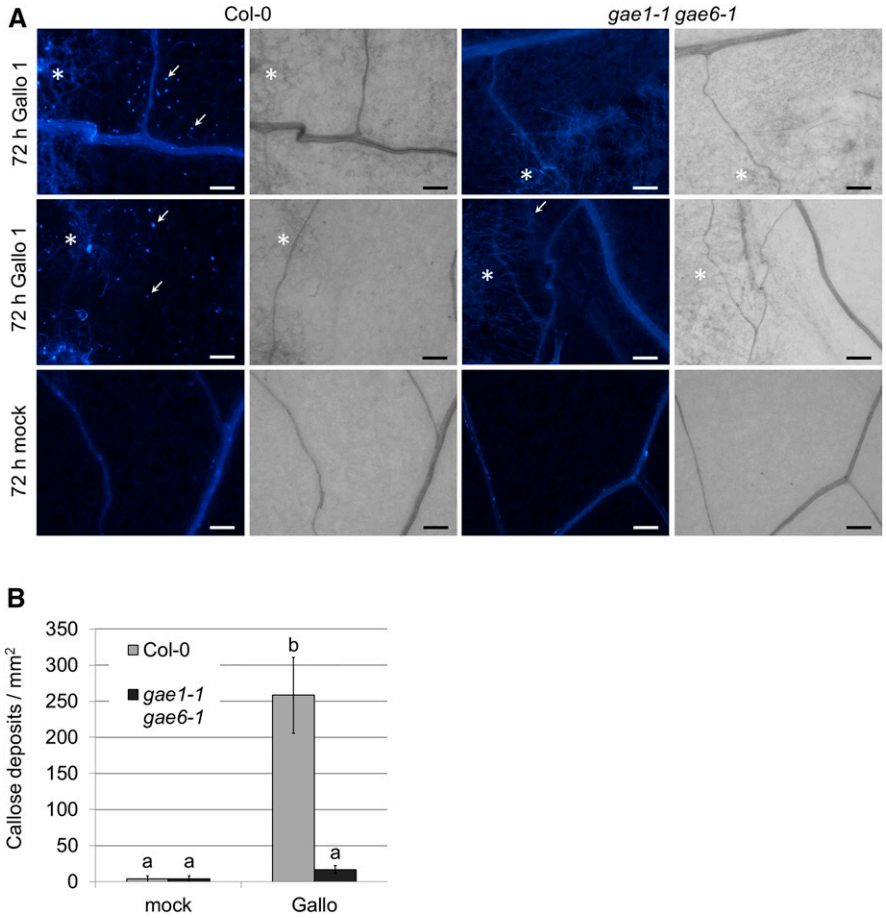

Figure 11. Gallo 1-Induced Callose Deposition Is Reduced in *gae1 gae6* Plants.

(A) Callose deposition in 4-week-old Col-0 and *gae1 gae6* plants. Plants were inoculated with *B. cinerea* isolate Gallo 1 (2.5×10^5 spores mL^{-1}) or mock inoculated with *B. cinerea* inoculation medium, and samples were collected after 72 h. Callose was stained with aniline blue and visualized using a Nikon Eclipse Ni-U microscope with a 4′,6-diamidino-2-phenylindole filter. Three leaves were stained per treatment. Asterisks indicate fungal hyphae, and arrows indicate representative callose spots. Bars = 100 μm.

(B) Quantification of callose deposition. Callose deposits were counted in 200 × 200-μm squares laid out across the images shown here. Bars represent means ± SE from six squares each. Letters indicate significantly different groups ($P < 0.05$) according to a *t* test analysis.

known to interact with pectin as part of its infection strategy. It secretes various pectin-degrading enzymes early during infection and requires some of these enzymes, including PG1, PG2, and PME1, for full virulence (ten Have et al., 1998; Valette-Collet et al., 2003; Kars et al., 2005b; Espino et al., 2010). Additionally, Arabidopsis plants expressing an antisense construct of the polygalacturonase inhibitor *PGIP1* are significantly more susceptible to *B. cinerea* (Ferrari et al., 2006). On the other hand, *Pma* ES4326 is not known to require cell wall degrading enzymes for full virulence even though it encodes two pectate lyase genes in its genome (PMA4326_07094 and PMA4326_04621; www.bacteria.ensembl.org). *B. cinerea* isolates are also known to be genetically quite diverse in their polygalacturonase loci, and genetic variability in *PG2* is associated with varying growth on pectin containing media (Rowe and Kliebenstein, 2007). Furthermore, the contribution of *PG1* and *PG2* to *B. cinerea* virulence seems to depend on the specific *B. cinerea* isolate and the host species (Kars et al., 2005a; Zhang and van Kan, 2013). *B. cinerea* isolates are also known to be differently sensitive to the antimicrobial secondary metabolite camalexin (Kliebenstein et al., 2005). In line with these observations, the susceptibility of *gae1 gae6* plants differed depending on the specific *B. cinerea* isolate. Whereas Fresa 525, Gallo 1, UK Razz, and KT grew better in *gae1 gae6*, we detected no difference in Acacia, Apple 517, DN, Grape, Pepper, or Rasp growth (Figure 6).

B. cinerea was shown to metabolize pectin and to possibly utilize GalA as a carbon source during in planta growth (Zhang et al., 2011; Zhang and van Kan, 2013). Our data show that *gae1 gae6* plants, which are reduced in GalA content, did allow enhanced growth of specific *B. cinerea* isolates, but no reduction in growth of any *B. cinerea* isolates tested was found. This suggests that utilization of pectin as a carbon source was not a contributing factor to alterations in *B. cinerea* susceptibility. It is possible that changes in the cell wall composition affect the structural integrity

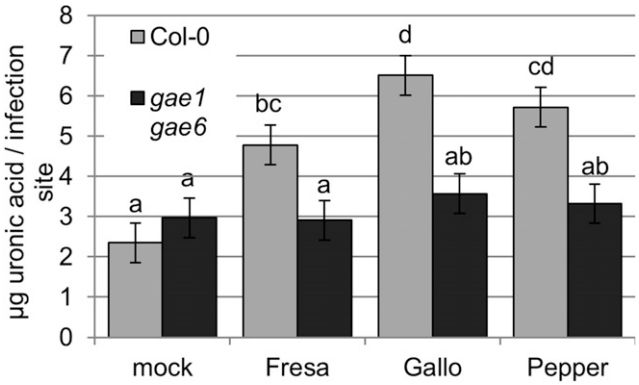

Figure 12. Less Soluble Pectin Accumulates in *B. cinerea*-Infected *gae1 gae6* Leaves.

Four-week-old Col-0 and *gae1 gae6* plants were inoculated with 10-µL droplets of the indicated *B. cinerea* isolate (2.5×10^5 spores mL^{-1}) or mock inoculated with *B. cinerea* inoculation medium. Leaves were collected 48 h later. AIR was extracted from leaf samples and water added (20 µL/infection site) to extract soluble pectin fragments. Samples were vortexed for 7 h and centrifuged at 12,000*g*, and the uronic acid concentration of the supernatant was measured. Data from nine biological replicates were combined using a mixed linear model. Means ± SE are shown. Letters indicate significant differences ($q < 0.05$).

of the wall and affect hyphal penetration of specific *B. cinerea* isolates. However, OGs (small HG fragments) are likely released during the infection process (Ferrari et al., 2013). OGs function as damage-associated molecular patterns and initiate immune responses in Arabidopsis (Ferrari et al., 2013). Treatment of Arabidopsis with OGs having a degree of polymerization of 10 to 15 sugar subunits was previously shown to enhance resistance to *B. cinerea* (Ferrari et al., 2007). We showed that pretreatment with OGs or macerozyme-induced enhanced immunity to *B. cinerea* isolate Gallo 1 in wild-type Col-0, but only OGs, and not macerozyme, induced immunity in *gae1 gae6* (Figure 13). Our data suggest *gae1 gae6* plants, which have reduced pectin content, may release less OGs and that this reduction leads to the increased susceptibility to *B. cinerea*.

Consistently, we found that macerozyme treatment released less soluble pectin from *gae1 gae6* cell walls than from wild-type walls. Fractions containing soluble pectin released from *gae1 gae6* were also less active in inducing *PAD3* gene expression than the fractions released from wild-type walls (Figure 7). We also showed that less soluble pectin accumulated in *gae1 gae6* than in wild-type plants 48 h after treatment with *B. cinerea* (Figure 12).

We observed that loss of pectin leads to alterations in Arabidopsis immune signaling. Macerozyme treatment induced expression of *PAD3* and the SA marker genes *PR1* and *SID2* in wild-type Col-0 but not in *gae1 gae6*, whereas OG treatment led to increased *PAD3* and *SID2* expression in both the wild type and *gae1 gae6* (Figures 8 and 9). This suggests that although release of active soluble pectin in these plants might be altered, OG recognition is intact. In fact, cell walls isolated from *qua1*, another mutant known to be reduced in HG, released less OGs (degree of polymerization 1 to 6) than did wild-type cell walls upon endopolygalacturonase treatment (Bouton et al., 2002). This was also true for *gae1 gae6* cell walls, as macerozyme treatment of isolated *gae1 gae6* cell walls released less soluble pectin than treatment of Col-0 cell walls. Because the fraction from *gae1 gae6* plants was also less active in inducing *PAD3* expression (Figure 7), it seems possible that biologically active OGs were the active component inducing *PAD3* expression. Interestingly, expression of the JA marker genes *JAZ5* and *JAZ10* was higher in *gae1 gae6* than in wild-type mock-inoculated plants but was comparable to the wild type in untreated plants, suggesting that JA signaling in *gae1 gae6* is hyperresponsive (Figure 10; Supplemental Figure 11). This induction of JA signaling might be due to wounding stress incurred during the inoculation process. JA and SA signaling generally act antagonistically (Pieterse et al., 2012). Increased JA signaling activity might hence explain why mock- and macerozyme-treated *gae1 gae6* plants exhibited reduced expression of the SA marker *PR1* and why OG treatment induced expression of *SID2*, another SA marker, to a lower extent in *gae1 gae6* than in wild-type plants (Figure 9).

No single immune signaling component was found to be the sole contributor to the compromised immunity of *gae1 gae6* to specific *B. cinerea* isolates, such as Gallo 1 and Fresa 525. These isolates grew better on *pad3*, while growth of Pepper, another *B. cinerea* isolate that did not show altered virulence on *gae1 gae6*, was unaltered (Supplemental Figure 9). This suggested that differences in camalexin sensitivity of these *B. cinerea* isolates might account for the differences in *gae1 gae6* susceptibility. However, camalexin accumulation and *PAD3* expression were the same for wild-type Col-0 and *gae1 gae6* for the *B. cinerea* isolates Fresa 525 and Gallo 1 (Figure 8), which showed enhanced growth on *gae1 gae6* plants. It should be noted that *B. cinerea* virulence is often estimated by comparing lesion sizes. Lesion size and measurements of relative fungal growth by qPCR do not always show the same results. For example, although Denby et al. (2004) showed that Pepper causes larger lesions on *pad3* than on the wild type, this study showed that relative fungal growth of Pepper on *pad3* was unaltered.

We observed that callose deposition was strongly reduced in *gae1 gae6* plants 72 h after treatment with *B. cinerea* isolate Gallo 1 (Figure 11), possibly due to reduced release of active soluble pectin. Interestingly, OG-induced PTI to an unspecified isolate of *B. cinerea* was intact in the *pmr4* mutant, which does not produce callose (Galletti et al., 2008). Due to the high SA levels in *pmr4* plants (Nishimura et al., 2003) and the fact that different *B. cinerea* isolates vary both in induction of and reaction to defense responses (Kliebenstein et al., 2005; Rowe et al., 2010), we could not determine whether reduced callose deposition causes the increased susceptibility of *gae1 gae6* to *B. cinerea* isolate Gallo 1.

We did not observe any changes in *B. cinerea* growth either on *cev1*/*ixr1* plants, which are known to have constitutively high JA and OPDA levels (Ellis et al., 2002b) or on plants exogenously treated with MeJA (Supplemental Figure 9). Because plants were kept uncovered for 3 h after MeJA treatment, it is unclear how much MeJA was bioavailable in the plant. However, *JAZ10* expression was induced 3 h after spraying with MeJA (Supplemental Figure 10). Because pathogen growth generally depends on the combination of a multitude of immune signaling events, we conclude that multiple changes to the immune signaling in *gae1 gae6* together account for the altered *B. cinerea* growth phenotypes detected.

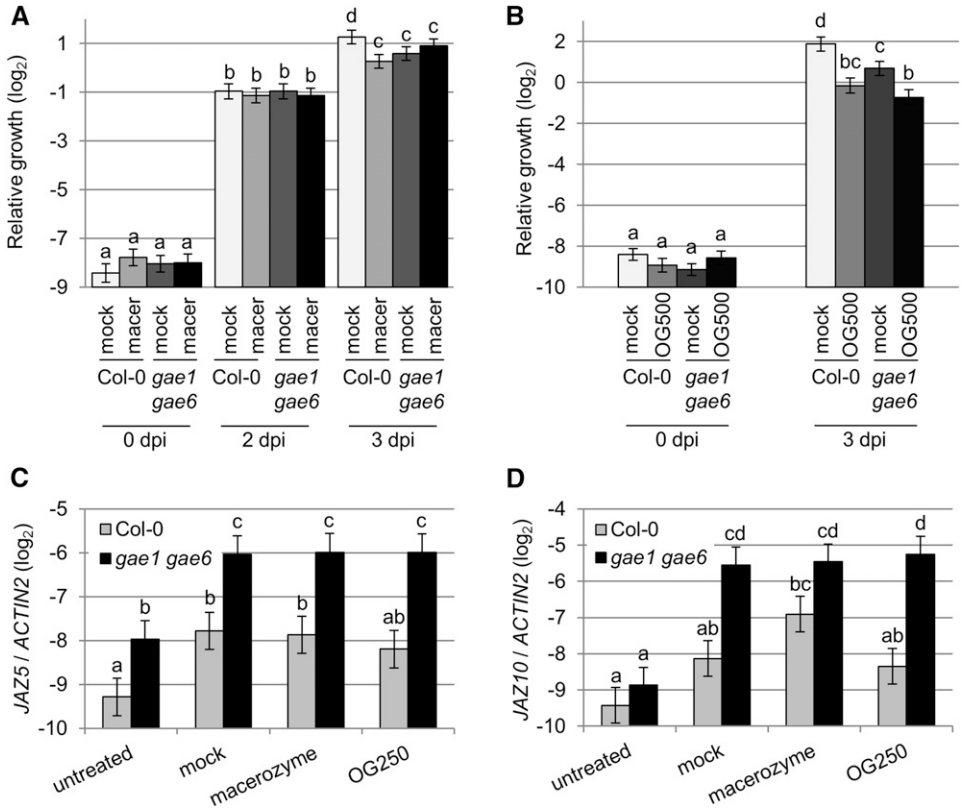

Figure 13. Macerozyme-Induced PTI Is Lost in *gae1 gae6* While OG-Induced PTI Is Unaltered.

(A) Macerozyme-induced PTI in Col-0 and *gae1 gae6* plants. Four-week-old plants were inoculated with 0.01% macerozyme or mock inoculated with boiled macerozyme and were infected with *B. cinerea* isolate Gallo 1 (2.5×10^5 spores mL^{-1}) 24 h later. Samples were collected immediately (0 dpi) and after two (2 dpi) and three (3 dpi) days. Data show mean ± SE of six to 14 biological replicates each combined using a linear model. Letters indicate significantly different groups ($q < 0.05$).

(B) OG-induced PTI in Col-0 and *gae1 gae6* plants. Four-week-old plants were inoculated with 500 µg mL^{-1} OGs and infected with *B. cinerea* as described in **(A)**. Six to eight biological experiments were performed.

(C) and **(D)** Expression of *JAZ5* **(C)** and *JAZ10* **(D)** was measured in untreated plants or 24 h after inoculation with water (mock), 0.01% macerozyme, or 250 µg mL^{-1} OGs. Data show mean $\log_2$ ratios to *ACTIN2* ± SE from three biological replicates combined using a mixed linear model. Letters indicate significantly different groups ($q < 0.05$). The q-value for comparison of *JAZ10* expression in the wild type and mutant after macerozyme treatment is 0.056.

We showed that expression of *GAE1* and *GAE6* is repressed by the bacterial hemibiotroph *Pma* ES4326. This repression did not occur in an *eds1* or *pad4* background or in *pbs3* at the 24-h time point (Figure 1; Supplemental Figure 1). During the Arabidopsis-*Pma* ES4326 interaction, the expression of many defense related genes is altered in a *PAD4*/*EDS1*-dependent fashion (Wang et al., 2008). Some of these expression changes require SA. *CBP60g* and *SARD1* are thought to act downstream of *PAD4* and *EDS1* but upstream of SA-dependent responses (Wang et al., 2011). *PBS3* is also thought to act downstream of *PAD4* and *EDS1* and upstream of SA, but the set of genes whose expression it affects is only partially overlapping with those affected by CBP60g/SARD1 (Wang et al., 2008, 2011). Thus, *GAE1* and *GAE6* repression is regulated by the part of the immune signaling network that requires *PAD4*/*EDS1* and *PBS3* but is independent of *CBP60g*/*SARD1* and SA. Because *EDS1*, *PAD4*, and *PBS3* are important components of the plant immune signaling network (Wiermer et al., 2005; Nobuta et al., 2007), one might conclude that repression of *GAE1* and *GAE6* may be part of the plant immune response to *Pma* ES4326. *B. cinerea* treatment also reduced *GAE1* and *GAE6* expression but this was mostly independent of *PAD4* (Figure 6); while both *Pma* ES4326 and *B. cinerea* repress *GAE1* and *GAE6* expression, the host signaling mechanisms responsible likely differ.

In summary, our data show that Arabidopsis *GAE1* and *GAE6* are required for pectin biosynthesis, leaf flexibility, and immunity to *Pma* ES4326 and to specific *B. cinerea* isolates. We used macerozyme, a commercial pectinase, to mimic the effect of *B. cinerea* pectinases. Macerozyme treatment released less pectin from *gae1 gae6* cell walls and induced less immune signaling in *gae1 gae6* plants. Less water-soluble pectin also accumulated in *B. cinerea*-infected *gae1 gae6* plants, and macerozyme-induced immunity to *B. cinerea* isolate Gallo 1 was reduced in these plants. We conclude that the reduced pectin content in these mutants may lead to reduced release of soluble pectin including active OGs during pathogen attack and that this compromises immunity.

METHODS

Plant Materials and Growth Conditions

Wild-type Columbia (Col-0) and all mutant plants (in Col-0 background) were grown on sterilized BM2 germinating mix (Berger) in a controlled environment chamber (Conviron) with a 12-h photoperiod under 100 μmol m^{-2} s^{-1} fluorescent illumination at 22°C and 75% relative humidity. Germplasm used is described in the Accession Numbers section at the end of Methods.

Data Analysis and Replicates

For biological replicates, samples were obtained from separate plant tissues and, in many cases, from plants grown in different flats. In some experiments, multiple technical replicates were measured per biological replicate. For statistical analysis, all technical replicates were averaged and the averages were considered one biological replicate. Independent experiments were performed at different times and often consisted of multiple biological replicates per experiment.

Data analysis was performed using mixed linear models in the R programming environment (Bates et al., 2015), unless otherwise indicated. Generally, genotypes, treatments, and time points were used as fixed effects, and replicate-specific effects, like different pots, flats, etc., were considered random effects. We reported P values, obtained from the mixed linear model, when less than 10 comparisons were performed and q-values for more than 10 comparisons to correct for multiple comparison testing. Q-values were calculated using the Benjamini-Hochberg procedure (Benjamini and Hochberg, 1995) unless specified otherwise.

Pathogen Strains, Growth Conditions, and Pathogen Growth Assays

Growth of *Pseudomonas syringae* pv *maculicola* ES4326 (*Pma* ES4326) and bacterial growth assays were performed as previously described (Bethke et al., 2014). For qRT-PCR assays, 4-week-old plants were inoculated with bacteria (OD_{600} = 0.002) or mock (5 mM $MgSO_4$). At least four leaves from two plants were collected at the indicated time points per biological replicate.

Prior to each experiment, *Botrytis cinerea* isolates were grown on 1× PDA medium (Difco) for 10 d at room temperature. All isolates used have been described previously (Rowe and Kliebenstein, 2007). The spores were washed from the surface of the plate using an inoculation medium (1× Gamborg's B-5 basal salt mixture [Sigma-Aldrich; G5768], 2% [w/v] glucose, and 10 mM phosphate buffer, pH 6.4), and fungal hyphae were removed from the suspension by filtering through four layers of cheesecloth. The concentration of spores was determined using a hemocytometer and adjusted to 2.5 × 10^5 spores mL^{-1}. Four-week-old *Arabidopsis thaliana* plants were inoculated by placing one 10-μL droplet of the *B. cinerea* spore solution or inoculation medium (mock) on the adaxial leaf surface of fully expanded leaves. Inoculated plants were kept at 100% relative humidity. Infection sites were collected at various time points using a cork borer. For qRT-PCR assays, at least four leaf discs from one plant were combined for each biological sample. For *B. cinerea* growth assays, at least 12 leaf discs from three to six plants were pooled per biological sample. Relative fungal growth was determined by measuring the abundance of a fungal gene relative to a plant gene as described below. In brief, DNA from infected tissue was extracted and equal amounts of total DNA were used to perform qPCR reactions using the *B. cinerea* cutinase A and the Arabidopsis *SK11* gene, respectively. Primers were described by Gachon and Saindrenan (2004) and are listed in Supplemental Table 1. Two technical replicates were combined for each biological replicate. *B. cinerea* is a necrotrophic fungal pathogen and may destroy plant DNA as disease progresses. However, decreases in the amount of plant DNA over the course of our experiments were only observed at late time points with very susceptible plants, so the qPCR assay is generally a reasonable estimate of fungal biomass (Supplemental Figure 16).

Treatment with Macerozyme or OGs

For PTI assays, 4-week-old plants either were inoculated with 0.01% (w/v) macerozyme R-10 (Yakult), a *Rhizopus* polygalacturonase (EC 3.2.1.15) that possesses high pectinase and hemicellulase activity, or were mock inoculated using heat-inactivated macerozyme. Other similar plants were either inoculated with 250 or 500 μg mL^{-1} OGs or mock inoculated with water. One day later, plants were infected with *B. cinerea* and samples were collected immediately (0 dpi) and 2 or 3 d later. To investigate the role of MeJA on *B. cinerea* growth, plants were sprayed with 1 mM MeJA in water with 0.01% (v/v) Tween 20. Covers were removed so that leaves could dry off before plants were inoculated with *B. cinerea* 3 h later. Samples were harvested at the indicated time points. For expression analysis and MAPK activation assays, plants were either inoculated with 100 μg mL^{-1} OGs or mock inoculated with water. OGs used for experiments described in Figures 8 to 10 and Supplemental Figure 12 were a kind gift from Simone Ferrari. OGs used in experiments described in Figure 13 and Supplemental Figures 11, 13, and 15 were prepared as previously described (Kohorn et al., 2014).

Expression Analysis

Leaf tissue from inoculated plants was harvested at the indicated time points, flash frozen, pulverized, and RNA extracted using Trizol (Invitrogen). Quantitative RT-PCR was performed using the SuperScript III Platinum SYBR Green One-Step quantitative RT-PCR kit (Invitrogen) and a Lightcycler 480 Real-Time PCR system (Roche) as previously described (Truman and Glazebrook, 2012). In brief, equal amounts of total RNA and a gene-specific primer were used for each reaction. The crossing point (Cp) was calculated using the second derivative max method provided with the Lightcycler software for each amplification curve. Each reaction was run with two technical replicates and the Cp values for these replicates were averaged. *ACTIN2* was used as a stably expressed reference gene. At least three biological replicates each were performed and analyzed using a mixed-linear model. RT-PCR was performed to verify T-DNA insertion lines using the One-Step RT-PCR kit (Qiagen) according to the manufacturer's instructions. The primers used can be found in Supplemental Table 1.

Electrolyte Leakage Assay

Fully expanded leaves of 4-week-old plants were inoculated with water (Milli-Q grade) using a needleless syringe. Leaf discs were collected using a cork borer and three leaf discs from one leaf were placed with the adaxial surface down onto 2 mL water in a 12-well cell culture plate. Conductivity was measured using a Horiba B-173 conductivity meter after 30 min and then the water was replaced. Conductivity was measured again 30 min later (1 h total) as indicated in Figure 3C. Six biological replicates each were performed in three independent experiments and means and standard errors were calculated. Two-sided *t* tests were performed for each time point.

3,3′-Diaminobenzidine and Aniline Blue Staining

Leaves from 4-week-old plants were either mock inoculated with *B. cinerea* inoculation medium or inoculated with 10-μL droplets of a *B. cinerea* spore solution (2.5 × 10^5 spores mL^{-1}) of the indicated isolates. Samples were collected 72 h later. For 3,3′-diaminobenzidine staining, two to five inoculated leaves were vacuum infiltrated with 3,3′-diaminobenzidine (1 mg mL^{-1} in water, pH 3.8) solution and stained overnight in the dark.

Leaves were destained using 100% ethanol at 65°C and then transferred to 50% (v/v) glycerol and photographed.

Callose was visualized by staining leaves with aniline blue as previously described (Adam and Somerville, 1996). Briefly, leaves were vacuum infiltrated with alcoholic lactophenol (1 volume of phenol:glycerol:lactic acid: water [1:1:1:1], mixed with two volumes of ethanol) and destained at 65°C. Next, leaves were moved through an alcohol gradient (50, 20, and 10% [v/v] ethanol) into water. The destained leaves were stained for 30 min in 150 mM K_2HPO_4 (pH 9.5) with 0.01% (w/v) aniline blue. Samples were mounted in water and examined using a Nikon Eclipse Ni-U microscope at 10× magnification using a 4′,6-diamidino-2-phenylindole filter (excitation at 325 to 375 nm; emission at 435 to 485 nm). For callose quantification, six 200 × 200-μm squares were counted for each sample type. Callose deposits per mm^2 were calculated and data analyzed using a *t* test. Note that there is an inherent uncertainty associated with such counts because callose deposits may not all be in focus at the same time.

MAPK Activity Assay

Fully expanded leaves of 4-week-old plants were inoculated with 0.01% macerozyme, 100 μg mL^{-1} OGs, 100 nM flg22, or water (mock). flg22, a peptide from bacterial flagella that induces immune responses, was used as a positive control for MAPK activation (Asai et al., 2002) and was purchased from EZBiolab. Samples were harvested 10 min later and immediately frozen in liquid nitrogen. Protein was extracted using an extraction buffer containing 25 mM Tris, pH 7.8, 75 mM NaCl, 1 mM DTT, 1 mM NaF, 0.5 mM Na_3VO_4, 0.1% (v/v) Tween 20, one cOmplete Mini protease inhibitor cocktail tablet (Roche), and one PhosSTOP phosphatase inhibitor cocktail tablet (Roche) per 10 mL buffer. Fifteen micrograms of total protein was electrophoresed on a 10% SDS-polyacrylamide gel and then blotted onto a PVDF membrane (Bio-Rad; 162-0177). Activated MAPKs were detected using p44/42 MAPK (Erk1/2) antibody (9102S Cell Signal, 1:2500 in TBST [20 mM Tris, pH 7.5, 150 mM NaCl, 0.1% (v/v) Tween 20]), anti-Rabbit IgG-HRP (1:15,000 in TBST and Sigma-Aldrich A6154), and ECL Plus substrate (Pierce; 32132). MPK3 and MPK6 were detected with an anti-MPK3 antibody (Sigma-Aldrich M8318, 1:2000 in TBST and 3% [w/v] milk) or an anti-MPK6 antibody (Sigma-Aldrich A7104, 1:6000 in TBST and 3% [w/v] milk), respectively. The secondary antibody and detection were the same as for the p44/42 antibody. Five independent experiments were performed.

Preparation of AIR, Pectin Extraction, and Uronic Acid Measurements

Fully expanded leaves from 4-week-old plants that were incubated for 48 h in the dark to reduce starch were harvested, flash frozen, and pulverized. AIR was extracted by washing ground material twice in 70% (v/v) ethanol, three times in a mixture of chloroform and methanol (1:1 [v/v]), and once in acetone (Gille et al., 2009) and was then air dried. Cell wall pectin was extracted from AIR with cell wall extraction buffer (50 mM Trizma and 50 mM CDTA, pH 7.2) at 95°C for 15 min. Samples were homogenized using a paint shaker (Harbil 5G-HD) and glass beads (3-mm diameter). For dot blot experiments, 500 μL of cell wall extraction buffer was used per 10 mg of AIR. Debris was precipitated by centrifugation for 10 min at 10,000*g*.

Total uronic acid content of pectin, extracted as described above using 500 μL of cell wall extraction buffer per 1 mg of AIR, was measured as described previously (Filisetti-Cozzi and Carpita, 1991; van den Hoogen et al., 1998). First, 36 μL of pectin extract were mixed with 4 μL of 4 M sulfamic acid. Then, 200 μL of sulfuric acid containing 120 mM sodium tetraborate was added and samples were incubated at 80°C for 1 h. Following cooling on ice, the optical density of samples was measured at 490 nm. Next, 40 μL of *m*-hydroxydiphenyl reagent (100 μL of *m*-hydroxydiphenyl in DMSO at 100 mg/mL mixed with 4.9 mL 80% [v/v] sulfuric acid just before use) was added and the samples were mixed. The optical density at 490 nm was measured again. The optical density before *m*-hydroxydiphenyl reagent addition was subtracted from the optical density measured after addition of the dye. The concentration of uronic acid was calculated using known amounts of GalA as a standard.

Release of Pectin from Arabidopsis Cell Walls Using Macerozyme

AIR preparations from leaves of 4-week-old plants were treated with 0.25% (w/v) macerozyme R-10 (Yakult) or water (mock) at a concentration of 100 μL per mg AIR. Samples were incubated for 3 h at room temperature on a vortex shaker and centrifuged for 10 min at 12,000*g*. Total uronic acid concentration of 5-fold diluted supernatants was determined for two technical replicates each. The concentration of uronic acid was calculated using known amounts of GalA as a standard. For subsequent qRT-PCR experiments, supernatants from multiple extractions were combined, boiled for 20 min to inactivate macerozyme, diluted 10-fold with water, and inoculated into 4-week-old Col-0 plants. Heat-inactivated, 10-fold diluted macerozyme solutions were used as mock treatment. Samples were collected 3 h later and *PAD3* expression was determined.

Release of Pectin from Arabidopsis Leaves Infected with *B. cinerea*

Fully expanded leaves of 4-week-old plants were either inoculated with up to five 10-μL droplets of *B. cinerea* spore solution (2.5×10^5 spores mL^{-1}) or mock inoculated with *B. cinerea* inoculation medium. For each biological replicate, leaves with a combined count of at least 20 infection sites were collected 48 h later. AIR was extracted as described above but plants were not dark-treated or freeze-dried and the first ethanol step was performed using 85% (v/v) ethanol. To extract soluble pectin fragments, AIR samples were mixed with water at a concentration of 20 μL per infection site, incubated for 7 h at room temperature on a vortex shaker, and centrifuged for 10 min at 12,000*g*. Total uronic acid concentration of supernatants was determined for two technical replicates each. The concentration of uronic acid was calculated using known amounts of GalA as a standard.

Measurement of Uronic Acids, Neutral Monosaccharides, and Cellulose Content in Cell Walls

Neutral sugars and uronic acids from noncellulosic polysaccharides in cell walls (AIR) were released by trifluoroacetic acid (TFA) hydrolysis. Approximately 1 mg of AIR was hydrolyzed with 2 M TFA at 121°C for 90 min. The TFA-soluble material was split into two equal parts, one for uronic acid and one for neutral sugar determination. The uronic acid content was determined by analyzing the hydrolyzate using a CarboPac PA200 anion-exchange column with an ICS-3000 Dionex chromatography system. The elution profile consisted of a linear gradient of 50 to 200 mM sodium acetate in 0.1 M NaOH in 10 min at 0.4 mL per min. Alditol acetate derivatives of neutral sugars were produced as described (York et al., 1985). In brief, monosaccharides in the hydrolyzate were reduced with $NaBH_4$ and peracetylated with acetic anhydride and pyridine at 121°C for 20 min. The generated alditol acetates were analyzed by gas chromatography-mass spectrometry. Crystalline cellulose was measured according to Updegraff (1969). After hydrolysis of noncellulosic polysaccharides from AIR with the Updegraff reagent (acetic acid:nitric acids:water, 8:1:2 [v/v]), the remaining pellet was hydrolyzed in 72% sulfuric acid. The resulting glucose quantity was determined by the anthrone method (Scott and Melvin 1953).

Dot Blot Experiments

Pectin solutions, extracted using 50 μL of cell wall extraction buffer per mg AIR, were serially diluted and nitrocellulose membranes were spotted with 1 μL of the diluted pectin solutions. Membranes were dried overnight,

blocked with 5% milk (w/v) in 1× PBS (8 g L^{-1} NaCl, 0.2 g L^{-1} KCl, 1.44 g L^{-1} Na_2HPO_4, and 0.24 g L^{-1} KH_2PO_4, pH 7.4), and probed with LM5 (Jones et al., 1997), LM6 (Willats et al., 1998), LM8 (Willats et al., 2004), LM19, and LM20 (Verhertbruggen et al., 2009a) or CCRC-M7 (Steffan et al., 1995) antibodies. LM series antibodies were diluted 1:250 and CCRC-M7 was diluted 1:500 in 5% milk powder (Nestle) in 1× PBS. For LM series antibodies, a goat anti-Rat HRP conjugated antibody (Bethyl A110-105P, 1:5000 diluted) and for CCRC-M7 an anti-Mouse IgG HRP conjugate (Promega W402B, 1:2500 diluted) was used as secondary antibody in 5% milk powder in 1× PBS. LM series antibodies were obtained from PlantProbes and CCRC-M7 from CarboSource. Membranes were washed after incubation with the primary and secondary antibodies with 1× PBS. Dot blots were developed using the ECL system (GE Healthcare; Amersham ECL prime). For quantification of signals, dot blot results on x-ray films were photographed using a CCD camera and intensities were measured using Image J's integrated density function. Locally adjusted background was subtracted. As the dynamic range of the signal on an x-ray film was narrow, nonlinearity in the measured values was corrected for each genotype in each biological replicate using the values from different dilutions in two technical replicates. We noticed that the residuals were not normally distributed and performed Box-Cox power transformation (Box and Cox, 1964) to obtain normally distributed values for the subsequent statistical analysis of the data. For LM19, Box-Cox selected power transformation was done to the power of 0.38th and for LM20 to the power 0.75th. After correction of the transformed measured values with the effect of the biological replicates, the values were fit to a linear model with the Arabidopsis genotype as the fixed effect. This linear model was used both to generate the plots in Figures 5B and 5D and to test significant differences.

Camalexin Measurements

Four-week-old plants were infected with *B. cinerea* and samples (three leaf disks from one plant each) were harvested at the indicated time points, flash-frozen, and pulverized. Each sample was extracted with 300 μL of 90% methanol (v/v). Fifty microliters of the extract was run on an Agilent Lichrocart 250-4 RP18e 5-μm column using an Agilent 1100 series HPLC. Camalexin was detected using a diode array at 330 nm and with a fluorescence detector at emission 318 nm/excitation 385 nm (Agilent). Separation was achieved using the following program with aqueous acetonitrile: 5-min gradient from 63 to 69% acetonitrile, 30-s gradient from 69 to 99% acetonitrile, 2 min at 99% acetonitrile, and a post-run equilibration of 3.5 min at 63% acetonitrile (Denby et al., 2004; Kliebenstein et al., 2005). Purified camalexin was used to produce a standard curve to identify and quantitate camalexin.

Accession Numbers

Microarray data used can be accessed at the NCBI Gene Expression Omnnibus (http://www.ncbi.nlm.nih.gov/geo/) under accession number GSE18978. Sequence information for all Arabidopsis genes described in this article can be found in TAIR (www.arabidopsis.org) using the following accession numbers: *PAD3* (*CYP71B15*, At3g26830), *SID2* (*ICS1*, At1g74710), *GAE1* (At4g30440), *GAE2* (At1g02000), *GAE3* (At4g00110), *GAE4* (At2g45310), *GAE5* (At4g12250), *GAE6* (At3g23820), *PR1* (At2g14610), *JAZ5* (At1g17380), *JAZ10* (At5g13220), *ACTIN2* (At3g18780), *PDF1.2a* (At5g44420), *PDF1.2b* (At2g26020), and *AtSK11* (At5g26751). The sequence of the *B. cinerea* cutinase *Bc-CutA* (Z69264) can be found in the DNA Data Bank of Japan (http://getentry.ddbj.nig.ac.jp). Germplasm used included *dde2-2* (At5g42650; von Malek et al., 2002), *pad3-1* (At3g26830; Zhou et al., 1999), *pad4-1* (At3g52430; Jirage et al., 1999), *sid2-2* (At1g74710; Wildermuth et al., 2001), *pbs3-2* (At5g13320, SALK_018225; Nobuta et al., 2007), *cbp60a-1* (At5g62570, SALK_124410; Truman et al., 2013), *cbp60g-1 sard1-2* (At5g26920, SALK_023199; At1g73805, SALK_052422; Wang et al., 2011), *cbp60a-1 cbp60g-1 sard1-2* (Truman et al., 2013), *gae1-1* (At4g30440, SALK_085554), *gae6-1* (At3g23280, SALK_104454), *gae6-2* (At3g23280, SALK_017191), *ixr1-1*/*cev1* (At5g05170; Ellis and Turner, 2001; Scheible et al., 2001). *eds1* plants were derived by introgression of the Landsberg *erecta eds1-2* allele into Col-0 that contains two copies of *EDS1* (At3g48090 and At3g48080; Bartsch et al., 2006), *mpk6-2* (At2g43790, SALK_073907; Liu and Zhang, 2004), *mpk3-DG* (At3g45640, a fast neutron deletion mutant; Miles et al., 2005), and *npr1-1* (At1g64280; Cao et al., 1997). T-DNA insertion lines were part of the SALK collection (Alonso et al., 2003) and were obtained from the ABRC.

Supplemental Data

Supplemental Figure 1. *Pma* ES4326-Induced Repression of *GAE1* and *GAE6* Expression Does Not Require *CBP60*s or *SID2*.

Supplemental Figure 2. Expression of *GAE* Family Members upon Treatment with *Pma* ES4326.

Supplemental Figure 3. Characterization of T-DNA Insertions in *GAE1* and *GAE6*.

Supplemental Figure 4. Mutant *gae6* and *gae1 gae6* Plants Have Brittle Leaves and Are Slightly Smaller Than Wild-Type Col-0 Plants.

Supplemental Figure 5. Cell Walls of *gae1 gae6* Plants Contain Less Uronic Acid Than Wild-Type Col-0 Cell Walls.

Supplemental Figure 6. Antibodies Raised against the RGI or XG Components of Pectin Show No Difference in Binding to *gae* Mutant and Col-0 Cell Walls.

Supplemental Figure 7. The Effect of *B. cinerea* Treatment on the Expression of *GAE* Family Genes.

Supplemental Figure 8. Treatment with 0.01% Macerozyme Does Not Cause Any Visible Damage to Col-0 Plants.

Supplemental Figure 9. *B. cinerea* Growth on Plants with Defects in Immune Signaling.

Supplemental Figure 10. MeJA-Induced Expression of the JA Marker Gene *JAZ10*.

Supplemental Figure 11. The Expression of the JA Marker Gene *JAZ5* Is Highly Responsive in *gae1 gae6* Plants.

Supplemental Figure 12. The Expression of *PDF1.2* Is Unaltered in *gae1 gae6* Plants.

Supplemental Figure 13. Macerozyme Treatment Activates MPK3 and MPK6.

Supplemental Figure 14. *B. cinerea*-Induced ROS Production in Wild-Type Col-0 and *gae1 gae6* Plants.

Supplemental Figure 15. OG-Induced PTI Using 250 μg mL^{-1} OGs.

Supplemental Figure 16. Abundance of Plant DNA in *B. cinerea*-Treated Plants.

Supplemental Table 1. Primers Used in This Study.

ACKNOWLEDGMENTS

We thank William Truman for helpful discussions, Simone Ferrari (Sapienza Universita di Roma) for the generous gift of OGs, Bruna Bucciarelli (USDA-ARS) for help with fluorescence microscopy, the ABRC for T-DNA insertion lines, Paul Knox's lab (University of Leeds) for LM5, LM6, LM8, LM19, and LM20 antibodies, and the Complex Carbohydrate Resource Center

(University of Georgia) for the CCRC-M7 antibody. Most of this work was funded by the Division of Chemical Sciences, Geosciences, and Biosciences, Office of Basic Energy Sciences of the U.S. Department of Energy through Grant DE-FG02-05ER15670 to J.G. This work was also supported by National Science Foundation Awards IOS 1339125 and IOS 1021861 to D.J.K., National Science Foundation Award IOS 1121425 to F.K., and the USDA National Institute of Food and Agriculture, Hatch project number CA-D-PLS-7033-H to D.J.K.

AUTHOR CONTRIBUTIONS

G.B. and J.G. designed the research. G.B., G.X., A.T., B.L., N.E.S., and N.H. performed research. D.J.K. provided tools. G.B., G.X., M.P., A.T., B.L., R.A.H., and F.K. analyzed data. G.B. and J.G. wrote the article with input from all authors.

Received May 6, 2015; revised December 11, 2015; accepted January 19, 2016; published January 26, 2016.

REFERENCES

Adam, L., and Somerville, S.C. (1996). Genetic characterization of five powdery mildew disease resistance loci in *Arabidopsis thaliana*. Plant J. **9:** 341–356.

Albersheim, P., Jones, T.M., and English, P.D. (1969). Biochemistry of the cell wall in relation to infective processes. Annu. Rev. Phytopathol. **7:** 171–194.

Alonso, J.M., et al. (2003). Genome-wide insertional mutagenesis of *Arabidopsis thaliana*. Science **301:** 653–657.

Asai, T., Tena, G., Plotnikova, J., Willmann, M.R., Chiu, W.L., Gomez-Gomez, L., Boller, T., Ausubel, F.M., and Sheen, J. (2002). MAP kinase signalling cascade in Arabidopsis innate immunity. Nature **415:** 977–983.

Bartsch, M., Gobbato, E., Bednarek, P., Debey, S., Schultze, J.L., Bautor, J., and Parker, J.E. (2006). Salicylic acid-independent ENHANCED DISEASE SUSCEPTIBILITY1 signaling in Arabidopsis immunity and cell death is regulated by the monooxygenase FMO1 and the Nudix hydrolase NUDT7. Plant Cell **18:** 1038–1051.

Bates, D., Machler, M., Bolker, B.M., and Walker, S.C. (2015). Fitting linear mixed-effects models using lme4. J. Stat. Softw. **67:** 1–48.

Benjamini, Y., and Hochberg, Y. (1995). Controlling the false discovery rate - a practical and powerful approach to multiple testing. J. Roy. Stat. Soc. B Met. **57:** 289–300.

Bethke, G., Grundman, R.E., Sreekanta, S., Truman, W., Katagiri, F., and Glazebrook, J. (2014). Arabidopsis PECTIN METHYLESTERASEs contribute to immunity against *Pseudomonas syringae*. Plant Physiol. **164:** 1093–1107.

Bouton, S., Leboeuf, E., Mouille, G., Leydecker, M.T., Talbotec, J., Granier, F., Lahaye, M., Höfte, H., and Truong, H.N. (2002). QUASIMODO1 encodes a putative membrane-bound glycosyltransferase required for normal pectin synthesis and cell adhesion in Arabidopsis. Plant Cell **14:** 2577–2590.

Box, G.E.P., and Cox, D.R. (1964). An analysis of transformations. J. R. Stat. Soc. B **26:** 211–252.

Cao, H., Glazebrook, J., Clarke, J.D., Volko, S., and Dong, X. (1997). The Arabidopsis NPR1 gene that controls systemic acquired resistance encodes a novel protein containing ankyrin repeats. Cell **88:** 57–63.

Carpita, N.C. (2011). Update on mechanisms of plant cell wall biosynthesis: how plants make cellulose and other (1→4)-β-D-glycans. Plant Physiol. **155:** 171–184.

Chisholm, S.T., Coaker, G., Day, B., and Staskawicz, B.J. (2006). Host-microbe interactions: shaping the evolution of the plant immune response. Cell **124:** 803–814.

Côté, F., and Hahn, M.G. (1994). Oligosaccharins: structures and signal transduction. Plant Mol. Biol. **26:** 1379–1411.

Denby, K.J., Kumar, P., and Kliebenstein, D.J. (2004). Identification of *Botrytis cinerea* susceptibility loci in *Arabidopsis thaliana*. Plant J. **38:** 473–486.

Denoux, C., Galletti, R., Mammarella, N., Gopalan, S., Werck, D., De Lorenzo, G., Ferrari, S., Ausubel, F.M., and Dewdney, J. (2008). Activation of defense response pathways by OGs and Flg22 elicitors in Arabidopsis seedlings. Mol. Plant **1:** 423–445.

Ellis, C., Karafyllidis, I., and Turner, J.G. (2002a). Constitutive activation of jasmonate signaling in an Arabidopsis mutant correlates with enhanced resistance to *Erysiphe cichoracearum*, *Pseudomonas syringae*, and *Myzus persicae.* Mol. Plant Microbe Interact. **15:** 1025–1030.

Ellis, C., Karafyllidis, I., Wasternack, C., and Turner, J.G. (2002b). The Arabidopsis mutant cev1 links cell wall signaling to jasmonate and ethylene responses. Plant Cell **14:** 1557–1566.

Ellis, C., and Turner, J.G. (2001). The Arabidopsis mutant cev1 has constitutively active jasmonate and ethylene signal pathways and enhanced resistance to pathogens. Plant Cell **13:** 1025–1033.

Espino, J.J., Gutiérrez-Sánchez, G., Brito, N., Shah, P., Orlando, R., and González, C. (2010). The *Botrytis cinerea* early secretome. Proteomics **10:** 3020–3034.

Ferrari, S., Galletti, R., Denoux, C., De Lorenzo, G., Ausubel, F.M., and Dewdney, J. (2007). Resistance to *Botrytis cinerea* induced in Arabidopsis by elicitors is independent of salicylic acid, ethylene, or jasmonate signaling but requires PHYTOALEXIN DEFICIENT3. Plant Physiol. **144:** 367–379.

Ferrari, S., Galletti, R., Vairo, D., Cervone, F., and De Lorenzo, G. (2006). Antisense expression of the *Arabidopsis thaliana* AtPGIP1 gene reduces polygalacturonase-inhibiting protein accumulation and enhances susceptibility to *Botrytis cinerea*. Mol. Plant Microbe Interact. **19:** 931–936.

Ferrari, S., Savatin, D.V., Sicilia, F., Gramegna, G., Cervone, F., and Lorenzo, G.D. (2013). Oligogalacturonides: plant damage-associated molecular patterns and regulators of growth and development. Front. Plant Sci. **4:** 49.

Filisetti-Cozzi, T.M., and Carpita, N.C. (1991). Measurement of uronic acids without interference from neutral sugars. Anal. Biochem. **197:** 157–162.

Gachon, C., and Saindrenan, P. (2004). Real-time PCR monitoring of fungal development in *Arabidopsis thaliana* infected by *Alternaria brassicicola* and *Botrytis cinerea*. Plant Physiol. Biochem. **42:** 367–371.

Galletti, R., Denoux, C., Gambetta, S., Dewdney, J., Ausubel, F.M., De Lorenzo, G., and Ferrari, S. (2008). The AtrbohD-mediated oxidative burst elicited by oligogalacturonides in Arabidopsis is dispensable for the activation of defense responses effective against *Botrytis cinerea*. Plant Physiol. **148:** 1695–1706.

Galletti, R., Ferrari, S., and De Lorenzo, G. (2011). Arabidopsis MPK3 and MPK6 play different roles in basal and oligogalacturonide- or flagellin-induced resistance against *Botrytis cinerea*. Plant Physiol. **157:** 804–814.

Gille, S., Hänsel, U., Ziemann, M., and Pauly, M. (2009). Identification of plant cell wall mutants by means of a forward chemical genetic approach using hydrolases. Proc. Natl. Acad. Sci. USA **106:** 14699–14704.

Grant, M.R., and Jones, J.D.G. (2009). Hormone (dis)harmony moulds plant health and disease. Science **324:** 750–752.

Gu, X., and Bar-Peled, M. (2004). The biosynthesis of UDP-galacturonic acid in plants. Functional cloning and characterization of Arabidopsis UDP-D-glucuronic acid 4-epimerase. Plant Physiol. **136:** 4256–4264.

Hahn, M.G., Darvill, A.G., and Albersheim, P. (1981). Host-pathogen interactions: XIX. The endogenous elicitor, a fragment of a plant cell wall polysaccharide that elicits phytoalexin accumulation in soybeans. Plant Physiol. **68:** 1161–1169.

Harholt, J., Suttangkakul, A., and Vibe Scheller, H. (2010). Biosynthesis of pectin. Plant Physiol. **153:** 384–395.

Hernández-Blanco, C., et al. (2007). Impairment of cellulose synthases required for Arabidopsis secondary cell wall formation enhances disease resistance. Plant Cell **19:** 890–903.

Jirage, D., Tootle, T.L., Reuber, T.L., Frost, L.N., Feys, B.J., Parker, J.E., Ausubel, F.M., and Glazebrook, J. (1999). *Arabidopsis thaliana* PAD4 encodes a lipase-like gene that is important for salicylic acid signaling. Proc. Natl. Acad. Sci. USA **96:** 13583–13588.

Jones, J.D.G., and Dangl, J.L. (2006). The plant immune system. Nature **444:** 323–329.

Jones, L., Seymour, G.B., and Knox, J.P. (1997). Localization of pectic galactan in tomato cell walls using a monoclonal antibody specific to (1->4)-beta-D-galactan. Plant Physiol. **113:** 1405–1412.

Kars, I., Krooshof, G.H., Wagemakers, L., Joosten, R., Benen, J.A.E., and van Kan, J.A.L. (2005b). Necrotizing activity of five *Botrytis cinerea* endopolygalacturonases produced in *Pichia pastoris*. Plant J. **43:** 213–225.

Kars, I., McCalman, M., Wagemakers, L., and VAN Kan, J.A.L. (2005a). Functional analysis of *Botrytis cinerea* pectin methylesterase genes by PCR-based targeted mutagenesis: Bcpme1 and Bcpme2 are dispensable for virulence of strain B05.10. Mol. Plant Pathol. **6:** 641–652.

Kim, S.J., Zemelis, S., Keegstra, K., and Brandizzi, F. (2015). The cytoplasmic localization of the catalytic site of CSLF6 supports a channeling model for the biosynthesis of mixed-linkage glucan. Plant J. **81:** 537–547.

Kliebenstein, D.J., Rowe, H.C., and Denby, K.J. (2005). Secondary metabolites influence Arabidopsis/Botrytis interactions: variation in host production and pathogen sensitivity. Plant J. **44:** 25–36.

Kohorn, B.D., Kohorn, S.L., Saba, N.J., and Martinez, V.M. (2014). Requirement for pectin methyl esterase and preference for fragmented over native pectins for wall-associated kinase-activated, EDS1/PAD4-dependent stress response in Arabidopsis. J. Biol. Chem. **289:** 18978–18986.

Liepman, A.H., Wightman, R., Geshi, N., Turner, S.R., and Scheller, H.V. (2010). Arabidopsis - a powerful model system for plant cell wall research. Plant J. **61:** 1107–1121.

Liu, Y., and Zhang, S. (2004). Phosphorylation of 1-aminocyclopropane-1-carboxylic acid synthase by MPK6, a stress-responsive mitogen-activated protein kinase, induces ethylene biosynthesis in Arabidopsis. Plant Cell **16:** 3386–3399.

Loewus, F.A., and Murthy, P.P.N. (2000). Myo-inositol metabolism in plants. Plant Sci. **150:** 1–19.

Miles, G.P., Samuel, M.A., Zhang, Y., and Ellis, B.E. (2005). RNA interference-based (RNAi) suppression of AtMPK6, an Arabidopsis mitogen-activated protein kinase, results in hypersensitivity to ozone and misregulation of AtMPK3. Environ. Pollut. **138:** 230–237.

Mohnen, D. (2008). Pectin structure and biosynthesis. Curr. Opin. Plant Biol. **11:** 266–277.

Mølhøj, M., Verma, R., and Reiter, W.D. (2004). The biosynthesis of D-Galacturonate in plants. functional cloning and characterization of a membrane-anchored UDP-D-Glucuronate 4-epimerase from Arabidopsis. Plant Physiol. **135:** 1221–1230.

Mouille, G., Ralet, M.C., Cavelier, C., Eland, C., Effroy, D., Hématy, K., McCartney, L., Truong, H.N., Gaudon, V., Thibault, J.F., Marchant, A., and Höfte, H. (2007). Homogalacturonan synthesis in *Arabidopsis thaliana* requires a Golgi-localized protein with a putative methyltransferase domain. Plant J. **50:** 605–614.

Nishimura, M.T., Stein, M., Hou, B.H., Vogel, J.P., Edwards, H., and Somerville, S.C. (2003). Loss of a callose synthase results in salicylic acid-dependent disease resistance. Science **301:** 969–972.

Nobuta, K., Okrent, R.A., Stoutemyer, M., Rodibaugh, N., Kempema, L., Wildermuth, M.C., and Innes, R.W. (2007). The GH3 acyl adenylase family member PBS3 regulates salicylic acid-dependent defense responses in Arabidopsis. Plant Physiol. **144:** 1144–1156.

Parsons, H.T., et al. (2012). Isolation and proteomic characterization of the Arabidopsis Golgi defines functional and novel components involved in plant cell wall biosynthesis. Plant Physiol. **159:** 12–26.

Pattathil, S., et al. (2010). A comprehensive toolkit of plant cell wall glycan-directed monoclonal antibodies. Plant Physiol. **153:** 514–525.

Pieterse, C.M.J., Van der Does, D., Zamioudis, C., Leon-Reyes, A., and Van Wees, S.C.M. (2012). Hormonal modulation of plant immunity. Annu. Rev. Cell Dev. Biol. **28:** 489–521.

Puhlmann, J., Bucheli, E., Swain, M.J., Dunning, N., Albersheim, P., Darvill, A.G., and Hahn, M.G. (1994). Generation of monoclonal antibodies against plant cell-wall polysaccharides. I. Characterization of a monoclonal antibody to a terminal alpha-(1–>2)-linked fucosyl-containing epitope. Plant Physiol. **104:** 699–710.

Rowe, H.C., and Kliebenstein, D.J. (2007). Elevated genetic variation within virulence-associated *Botrytis cinerea* polygalacturonase loci. Mol. Plant Microbe Interact. **20:** 1126–1137.

Rowe, H.C., Walley, J.W., Corwin, J., Chan, E.K.F., Dehesh, K., and Kliebenstein, D.J. (2010). Deficiencies in jasmonate-mediated plant defense reveal quantitative variation in *Botrytis cinerea* pathogenesis. PLoS Pathog. **6:** e1000861.

Scheible, W.R., Eshed, R., Richmond, T., Delmer, D., and Somerville, C. (2001). Modifications of cellulose synthase confer resistance to isoxaben and thiazolidinone herbicides in Arabidopsis Ixr1 mutants. Proc. Natl. Acad. Sci. USA **98:** 10079–10084.

Scheller, H.V., and Ulvskov, P. (2010). Hemicelluloses. Annu. Rev. Plant Biol. **61:** 263–289.

Scott, T.A., and Melvin, E.H. (1953). Determination of dextran with anthrone. Anal. Chem. **25:** 1656–1661.

Seifert, G.J. (2004). Nucleotide sugar interconversions and cell wall biosynthesis: how to bring the inside to the outside. Curr. Opin. Plant Biol. **7:** 277–284.

Steffan, W., Kovác, P., Albersheim, P., Darvill, A.G., and Hahn, M.G. (1995). Characterization of a monoclonal antibody that recognizes an arabinosylated (1–>6)-beta-D-galactan epitope in plant complex carbohydrates. Carbohydr. Res. **275:** 295–307.

Tao, Y., Xie, Z., Chen, W., Glazebrook, J., Chang, H.S., Han, B., Zhu, T., Zou, G., and Katagiri, F. (2003). Quantitative nature of Arabidopsis responses during compatible and incompatible interactions with the bacterial pathogen *Pseudomonas syringae*. Plant Cell **15:** 317–330.

Tenhaken, R., and Thulke, O. (1996). Cloning of an enzyme that synthesizes a key nucleotide-sugar precursor of hemicellulose biosynthesis from soybean: UDP-glucose dehydrogenase. Plant Physiol. **112:** 1127–1134.

ten Have, A., Mulder, W., Visser, J., and van Kan, J.A.L. (1998). The endopolygalacturonase gene Bcpg1 is required for full virulence of *Botrytis cinerea.* Mol. Plant Microbe Interact. **11:** 1009–1016.

Truman, W., and Glazebrook, J. (2012). Co-expression analysis identifies putative targets for CBP60g and SARD1 regulation. BMC Plant Biol. **12:** 216.

Truman, W., Sreekanta, S., Lu, Y., Bethke, G., Tsuda, K., Katagiri, F., and Glazebrook, J. (2013). The CALMODULIN-BINDING PROTEIN60 family includes both negative and positive regulators of plant immunity. Plant Physiol. **163:** 1741–1751.

Updegraff, D.M. (1969). Semimicro determination of cellulose in biological materials. Anal. Biochem. **32:** 420–424.

Usadel, B., Schlüter, U., Mølhøj, M., Gipmans, M., Verma, R., Kossmann, J., Reiter, W.D., and Pauly, M. (2004). Identification and characterization of a UDP-D-glucuronate 4-epimerase in Arabidopsis. FEBS Lett. **569:** 327–331.

Valette-Collet, O., Cimerman, A., Reignault, P., Levis, C., and Boccara, M. (2003). Disruption of *Botrytis cinerea* pectin methylesterase gene *Bcpme1* reduces virulence on several host plants. Mol. Plant Microbe Interact. **16:** 360–367.

van den Hoogen, B.M., van Weeren, P.R., Lopes-Cardozo, M., van Golde, L.M.G., Barneveld, A., and van de Lest, C.H.A. (1998). A microtiter plate assay for the determination of uronic acids. Anal. Biochem. **257:** 107–111.

Verhertbruggen, Y., Marcus, S.E., Haeger, A., Ordaz-Ortiz, J.J., and Knox, J.P. (2009a). An extended set of monoclonal antibodies to pectic homogalacturonan. Carbohydr. Res. **344:** 1858–1862.

Verhertbruggen, Y., Marcus, S.E., Haeger, A., Verhoef, R., Schols, H.A., McCleary, B.V., McKee, L., Gilbert, H.J., and Knox, J.P. (2009b). Developmental complexity of arabinan polysaccharides and their processing in plant cell walls. Plant J. **59:** 413–425.

Vogel, J.P., Raab, T.K., Schiff, C., and Somerville, S.C. (2002). PMR6, a pectate lyase-like gene required for powdery mildew susceptibility in Arabidopsis. Plant Cell **14:** 2095–2106.

Vogel, J.P., Raab, T.K., Somerville, C.R., and Somerville, S.C. (2004). Mutations in PMR5 result in powdery mildew resistance and altered cell wall composition. Plant J. **40:** 968–978.

von Malek, B., van der Graaff, E., Schneitz, K., and Keller, B. (2002). The Arabidopsis male-sterile mutant dde2-2 is defective in the ALLENE OXIDE SYNTHASE gene encoding one of the key enzymes of the jasmonic acid biosynthesis pathway. Planta **216:** 187–192.

Wang, L., Mitra, R.M., Hasselmann, K.D., Sato, M., Lenarz-Wyatt, L., Cohen, J.D., Katagiri, F., and Glazebrook, J. (2008). The genetic network controlling the Arabidopsis transcriptional response to *Pseudomonas syringae* pv. maculicola: roles of major regulators and the phytotoxin coronatine. Mol. Plant Microbe Interact. **21:** 1408–1420.

Wang, L., Tsuda, K., Truman, W., Sato, M., Nguyen, V., Katagiri, F., and Glazebrook, J. (2011). CBP60g and SARD1 play partially redundant critical roles in salicylic acid signaling. Plant J. **67:** 1029–1041.

Wiermer, M., Feys, B.J., and Parker, J.E. (2005). Plant immunity: the EDS1 regulatory node. Curr. Opin. Plant Biol. **8:** 383–389.

Wildermuth, M.C., Dewdney, J., Wu, G., and Ausubel, F.M. (2001). Isochorismate synthase is required to synthesize salicylic acid for plant defence. Nature **414:** 562–565.

Willats, W.G.T., Marcus, S.E., and Knox, J.P. (1998). Generation of monoclonal antibody specific to (1–>5)-alpha-L-arabinan. Carbohydr. Res. **308:** 149–152.

Willats, W.G.T., et al. (2004). A xylogalacturonan epitope is specifically associated with plant cell detachment. Planta **218:** 673–681.

Windram, O., et al. (2012). Arabidopsis defense against *Botrytis cinerea*: chronology and regulation deciphered by high-resolution temporal transcriptomic analysis. Plant Cell **24:** 3530–3557.

Yan, S., and Dong, X. (2014). Perception of the plant immune signal salicylic acid. Curr. Opin. Plant Biol. **20:** 64–68.

York, W.S., Darvill, A.G., Mcneil, M., and Albersheim, P. (1985). Structure of plant cell walls. 16. 3-Deoxy-D-manno-2-octulosonic acid (Kdo) is a component of rhamnogalacturonan-II, a pectic polysaccharide in the primary cell walls of plants. Carbohydr. Res. **138:** 109–126.

Zablackis, E., Huang, J., Müller, B., Darvill, A.G., and Albersheim, P. (1995). Characterization of the cell-wall polysaccharides of *Arabidopsis thaliana* leaves. Plant Physiol. **107:** 1129–1138.

Zandleven, J., Sørensen, S.O., Harholt, J., Beldman, G., Schols, H.A., Scheller, H.V., and Voragen, A.J. (2007). Xylogalacturonan exists in cell walls from various tissues of *Arabidopsis thaliana*. Phytochemistry **68:** 1219–1226.

Zhang, L., Thiewes, H., and van Kan, J.A.L. (2011). The D-galacturonic acid catabolic pathway in *Botrytis cinerea*. Fungal Genet. Biol. **48:** 990–997.

Zhang, L., and van Kan, J.A.L. (2013). *Botrytis cinerea* mutants deficient in D-galacturonic acid catabolism have a perturbed virulence on *Nicotiana benthamiana* and Arabidopsis, but not on tomato. Mol. Plant Pathol. **14:** 19–29.

Zhou, N., Tootle, T.L., and Glazebrook, J. (1999). Arabidopsis PAD3, a gene required for camalexin biosynthesis, encodes a putative cytochrome P450 monooxygenase. Plant Cell **11:** 2419–2428.